BRNO UNIVERSITY OF TECHNOLOGY
VYSOKÉ UČENÍ TECHNICKÉ V BRNĚ

FACULTY OF CHEMISTRY
FAKULTA CHEMICKÁ

INSTITUTE OF CHEMISTRY AND TECHNOLOGY OF ENVIRONMENTAL PROTECTION
ÚSTAV CHEMIE A TECHNOLOGIE OCHRANY ŽIVOTNÍHO PROSTŘEDÍ

DETERMINATION OF TITANIUM DIOXIDE NANOPARTICLES IN PERSONAL CARE PRODUCTS
DETERMINATION OF TITANIUM DIOXIDE NANOPARTICLES IN PERSONAL CARE PRODUCTS

MASTER'S THESIS
DIPLOMOVÁ PRÁCE

AUTHOR — **Bc. Juraj Košík**
AUTOR PRÁCE

SUPERVISOR — **prof. RNDr. Milada Vávrová, CSc.**
VEDOUCÍ PRÁCE

BRNO 2016

Vysoké učení technické v Brně
Fakulta chemická
Purkyňova 464/118, 61200 Brno

Zadání diplomové práce

Číslo diplomové práce:	**FCH-DIP0954/2015**	Akademický rok: **2015/2016**
Ústav:	Ústav chemie a technologie ochrany životního prostředí	
Student(ka):	**Bc. Juraj Košík**	
Studijní program:	Chemie a technologie ochrany životního prostředí (N2805)	
Studijní obor:	Chemie a technologie ochrany životního prostředí (2805T002)	
Vedoucí práce	**prof. RNDr. Milada Vávrová, CSc.**	
Konzultanti:		

Název diplomové práce:

Determination of titanium dioxide nanoparticles in personal care products

Zadání diplomové práce:

Process literature review aimed on extraction methods for metal oxide nanoparticles in personal care products.
Suggest the method for extraction of TiO2 nanoparticles from personal care products.
Test and optimization of chosen method for the products and standards and determine its metrological parameters.
Interpretation of obtained results.

Termín odevzdání diplomové práce: 19.5.2016

Diplomová práce se odevzdává v děkanem stanoveném počtu exemplářů na sekretariát ústavu a v elektronické formě vedoucímu diplomové práce. Toto zadání je přílohou diplomové práce.

Bc. Juraj Košík	prof. RNDr. Milada Vávrová, CSc.	prof. RNDr. Milada Vávrová, CSc.
Student(ka)	Vedoucí práce	Ředitel ústavu

V Brně, dne 31.1.2016

prof. Ing. Martin Weiter, Ph.D.
Děkan fakulty

ABSTRACT

The following master thesis deals with extraction of titanium dioxide nanoparticles (TiO_2 NPs) from consumer care products, concretely sunscreens, and subsequent characterization of these particles. TiO_2 nanoparticles are present in an increasing number of commercially available products. Therefore, there is an increasing need to evaluate the potential fate and indirect exposure of TiO_2 NPs of different sizes and shapes and investigate their entire life cycle. Feasibility of using ultrafiltration and ultracentrifugation as an extraction method were investigated. Two extraction method for extracting TiO_2 nanoparticles were developed and applied to sunscreen samples. Extracted particles can be used for ecotoxicological and mesocosmos experiments. Secondly, size of extracted particles was determined using dynamic light scattering (DLS) and transmission electron microscopy (TEM).

KEYWORDS

Sunscreen, TiO_2 nanoparticles, ultracentrifugation, ultrafiltration, inductively coupled plasma with mass spectrometry (ICP-MS), scanning electron microscopy (SEM), transition electron microscopy (TEM), dynamic light scattering (DLS), nanoparticle tracking analysis (NTA).

ABSTRAKT

Předkládaná diplomová práce se zabývá extrakcí nanočástic oxidu titaničitého z produktů osobní péče, konkrétně opalovacích krémů a následnou charakterizací těchto částic. Počet komerčně dostupných produktů s obsahem nanočástic TiO_2 se neustále zvyšuje a to se sebou přináší potřebu vyhodnotit potenciální osud a nepřímou expozici TiO_2 nanošástic o různých velikostí a tvarů a zkoumat jejich celý životní cyklus. Bylo zkoumáno použití ultrafiltrace a ultracentrifugace jako extrakční metody. Dvě metody pro extrakci TiO_2 nanočástic byly vyvinuty a aplikovány na vzorky opalovacích krémů. Extrahované částice mohou být použity pro ekotoxikologické studie, případně experimenty v mesokosmu. Velikost částic byla stanovena pomocí metody dynamického rozptylu světla a transmisní elektronové mikroskopie.

KLÍČOVÁ SLOVA

Opalovací krém, nanočástice TiO_2, ultracentrifugace, ultrafiltrace, indukčně vázané plazma s hmotnostní spektrometrií (ICP-MS), skenovací elektronová mikroskopie (SEM), tranzitní elektronová mikroskopie (TEM), metoda dynamického rozptylu světla (DLS) analýza trajektorie pohybu nanočástic (NTA).

KOŠÍK, J. *Determination of titanium dioxide nanoparticles in personal care products*. Brno: Vysoké učení technické v Brně, Fakulta chemická, 2016. 75 s. Vedoucí diplomové práce prof. RNDr. Milada Vávrová, CSc..

DECLARATION

I declare that the master thesis has been elaborated by me and that all the quotations from the used literary sources are accurate and complete. The content of master thesis is the property of the Faculty of Chemistry of Brno University of Technology and all commercial uses are allowed only if approved by both the supervisor of thesis and the dean of the Faculty of Chemistry, Brno University of Technology

……

student´s signature

PROHLÁŠENÍ

Prohlašuji, že jsem bakalářskou práci vypracoval samostatně a že všechny použité literární zdroje jsem správě a úplně citoval. Bakalářská práce je z hlediska obsahu majetkem Fakulty chemické Vysokého učení technického v Brně (FCH VUT) a může být využita ke komerčním účelům jen se souhlasem vedoucího bakalářské práce a děkana FCH VUT.

……

podpis studenta

ACKNOWLEDGEMENT

I would like to say thank you to my supervisor at Brno University of Technology, prof. RNDr. Milada Vávrová, CSc. for her valuable and scientific advices.

Dr. Jiří Kučerík, the associated professor of physical chemistry is acknowledged. Thanks to him and his international contacts I was allowed to travel to Landau and elaborate the master thesis there.

Another really gorgeous thank you goes to my supervisor at University of Koblenz and Landau, Dr. Allan Philippe, for supervising me trough whole thesis work in laboratory and for his scientific leading me through whole work.

I would like to say thanks to whole environmental and soil chemistry working group at University of Koblenz and Landau, who accepted me as a part of family, they also helped in chemistry field and made my time in Germany were pleasant.

Laboratory for Electron Microscopy at Karlsruhe Institute of Technology (*KIT*), *where all my TEM measurements were done, is acknowledged too.*

Last but not least thank you goes also to my family who supported me in financial and mental way.

1. CONTENT

2. INTRODUCTION

The dramatic increase in use of engineered nanoparticles in wide range of applications that promise great benefits for society causes also increasing concern of significant adverse effects of these nanoparticles for human and the environment [1, 2] With rapidly developing field of nanotechnology therefore the interest of scientists in this field is growing last years. Engineered nanoparticles are used in personal care products, pharmaceuticals, electronics, tires, disposable materials, food etc. [3].

Research suggests that toxicological and adverse effects related with nanoparticles are strongly dependent on the particle size [4, 5]. The smaller the particles are, the greater potential of adverse effect due to higher ability of smaller particles to penetrate human body or biological membranes, respectively [3]. As a result there is a great need to determine the size of wide used nanoparticles. According to the recommendation of European Union Commission number 2011/696/EU definition of nanomaterial is: a natural, incidental or manufactured material containing particles, in an unbound state or as an aggregate or as an agglomerate and where, for 50 % or more of the particles in the number size distribution, one or more external dimensions is in the size range 1 – 100 nm [6].

Recently the popularity of titanium dioxide nanoparticles as a content of mineral sunscreens have grown due to their physical ability to reflect and scatter as UVA as UVB radiations. In addition they do not disrupt the endocrine system compared to some chemical UV filters [7].

Since small particles can cross biological membranes whereas larger particles normally cannot, it is necessary to develop a method that is able to detect primary (non-aggregated) TiO_2 nanoparticles in commercially available sunscreens [8]. Electron microscopy is often used in studies of nanoparticles due to possibility to identify the presence of these particles and providing useful information of size distribution and other measurable properties [9, 10]. However, electron microscopy is technique which is not always available and other analytical techniques should be investigated for possibility to measure size distribution of particles.

Firstly there is need for developing extracting method for TiO_2 nanoparticles from sunscreen lotion matrix because isolated NPs could be better handled. Secondly, the developed efficient extraction procedure provides us extracted TiO_2 NPs from sunscreens which could be used for ecotoxicological tests in the frame of project InterNano.

In this study ability to determine primary particle size of extracted particles using dynamic dight scattering (DLS), nanoparticle tracking analysis (NTA) and hydrodynamic chromatography coupled with inductively coupled plasma-mass spectrometry (HDC-ICP-MS) techniques was investigated. The results of size distribution were verified by measurement obtained with Transmission Electron Microscopy (TEM).

Developed methodology of extraction and subsequently size characterization method was applied to eleven commercially available sunscreens with sun protection factors (SPF) ≥ 30. Total TiO_2 content in sunscreen, extraction efficiency and particle size distribution of TiO_2 nanoparticles were determined for each product.

3. THEORETICAL PART

3.1 Sun risk and protection

Ultraviolet (UV) radiation from the sun is a constant presence on the earth. This harmful radiation can permanently damage the largest organ of the human body, the skin. Sunburn is the most obvious sign of this damage. It can range from just irritation to a serious burn requiring medical treatment or even hospitalization. A sunburn can take days to heal and can result in permanent mottling of the skin, age spots, and melanoma.

Skin can be protected by limiting exposure and covering the body. Two main basic types of sun protection formula in modern chemistry have been developed, sunscreen and sunblock. Sunscreen is a chemical solution, classified as a drug, which has properties to absorb sun rays before it can harm the skin. However, sunblock protects the skin by reflecting and scattering the UV radiation. For example zinc oxide is the most used sunblock. Although sunblocks are highly effective, it´s typically sticky creams makes it impractical for full body use [11, 12].

3.1.1 What is UV

UV radiation is part of the electromagnetic spectrum that reaches the earth from the sun. It has wavelengths shorter than visible light, making it invisible to the human eye. According the different wavelengths regions we distinguish 3 main types of UV rays that damage skin [13]:

- **UVA** is responsible for the majority of sunburns (wavelength range 320-400 nm).
- **UVB** penetrates deeper into the skin. It ages the skin, but contributes much less towards sunburn (wavelength range 290-320 nm).
- **UVC** is the most dangerous of all, but fortunately it is completely filtered out by the ozone layer and doesn’t reach the earth's surface (wavelength range 100-290 nm).

Penetration abilities of these 3 types of UV rays are shown in *fig. 1*.

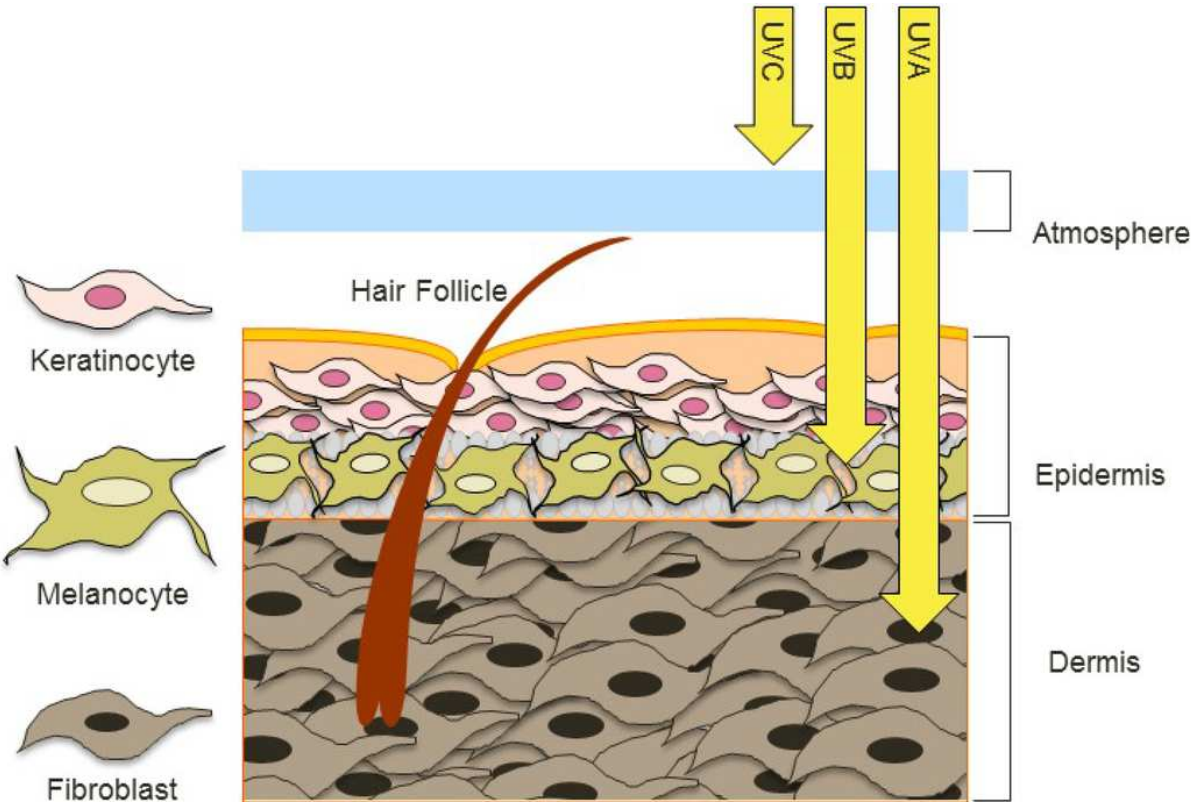

Figure 1 – penetration ability of UVA, UVB and UVC rays [14].

UVB is characterized as a mutagen relatively for a long time, but recent studies point out on increasing role of UVA as a carcinogen due to its pro-oxidative effects and other mechanisms. However, UVA is less able to induce melanin production compared to UVB rays it has still high potential in melanoma formation.UVA can be one of the reasons of increased melanoma cases during the last several decades. Especially when we realize that, in the 1980s, only UVB-protecting sunscreens were used [15].

3.1.2 History of sun protection

Some past and present cultures often consider light-coloured skin more beautiful and attractive that dark one. For example, ancient Egyptians tried to avoid sun radiation from reaching the skin. Some of the ingredients used at that time have been rediscovered by modern chemistry. For example, gamma oryzanol extracted from rice bran is used in modern sunscreens as UV-absorbant [12]. The Egyptians also used jasmine, which can heal DNA at the cellular level in the skin, to recover skin damage. Next example is lupine extract which is used to lighten the skin, as ingredient was already used for that purpose at the time by the Egyptians [12, 15].

Before the discovery of UV light, people thought that sunburn is caused just by heat from sun. UV rays were discovered by Johann Wilhelm Ritter of Germany in 1801. His work was based

by previous work of Carl Wilhelm Scheele. Ritter tried to measure the effects of light rays below the visible blue region, which led to the discovery of the UV spectrum. He called it "infraviolet". [17]

Two Germans, Karl Eilham Hausser und Wilhelm Vahle reported in 1922 that sunburn is caused by the part of the UV spectrum. The first commercially available sunscreen was produced in 1928 in the US as an emulsion made of PABA benzyl salicylate and benzyl cinnamate [18].

Increasing number of different sun protecting products created a demand for quality control. It was done in 1962 by Franz Greiter who developed a way to measure ability to block ultraviolet rays and it is known as the sun protection factor, or SPF [17, 19]. SPF is a measure of how much solar energy (UV radiation) is required to produce sunburn on protected skin relative to the amount of solar energy required to produce a sunburn on unprotected skin [20]. If skin of some person would normally burn after 10 minutes in the sun, applying an SPF 15 sunscreen would allow to this person stay in the sun without burning for approximately 15 times longer, so 150 minutes [21].

This is a rough estimate that depends on skin type, intensity of sunlight and amount of sunscreen used. SPF is actually a measure of protection from amount of UVB exposure and it is not meant to help determine duration of exposure.

3.1.3 Modern sunscreens

The most common sunscreens available on the market nowadays contain two forms of UV-filter: organic and inorganic filters. Those forms differ in skin protecting mechanism and each may be hazardous to human health. Organic filter products typically contain a combination of two and more of these active ingredients: oxybenzone, octinoxate, homosalate, octisalate, octocrylene and avobenzone [22]. Basic health characteristics of the most used sunscreen filters are shown in *table 2*.

Inorganic sunscreens use properties of zinc oxide and titanium dioxide. Some sunscreens combine organic and inorganic filters [22]. TiO_2 is the most used UV-filter in sunscreen and with the development of nanotechnology the TiO_2 is applied in form of particles of sizes in nano range [23].

Table 1 – basic health characteristics of the most used sunscreen filters.

Chemical	UV Range Covered*	Skin Penetration	Hormone Disruption	Skin Allergy	Others	Ref.
Oxybenzone	UVB, UVA2	Detected in almost American, found in mother´s milk, 1–9 % skin penetration in lab. studies	Acts like estrogen – alerts sperm production in animals, associated with endometriosis in woman	Relatively high rates of skin allergy		[24] [25]
Octinoxate	UVB	Found in mother´s milk, <1 % skin penetration in lab. studies	Hormone like activity – reproductive system, thyroid and behavioral changes in animal studies	Moderate rates of skin allergy		[24] [26]
Homosalate	UVB	Found in mother´s milk, <1 % skin penetration in lab. studies	Disrupts estrogen, androgen and progesterone	Not found	Toxic degradation products	[24] [27]
Octisalate	UVB	Skin penetration in lab. studies	No evidence of hormone disruption	Rarely reported skin allergy	Stabilizes avobenzone	[28]
Octocrylene	UVB	Found in mother´s milk, skin penetration in lab. studies	No evidence of hormone disruption	Relatively high rates of skin allergy		[24] [29]
Avobenzone	UVA1	Very low skin penetration	No evidence of hormone disruption	Relatively high rates of skin allergy		[26] [29]
TiO_2	UVB, UVA2	Skin penetration not founded	No evidence of hormone disruption	None	Inhalation concerns	[30] [31]
ZnO	UVB, UVA2 UVA1	Skin penetration <0,01 % in human volunteers	No evidence of hormone disruption	None	Inhalation concerns	[30] [32]

*ranges of UV radiation, UVB: 290-320 nm, UVA2: 320-340 nm and UVA1: 340-400 nm [11].

3.2 Titanium dioxide

TiO_2 belongs to the family of transition metal oxides. There are three known crystallographic structures of TiO_2 commonly found in nature: anatase, rutile and brookite. The structure of these three main phases is well characterized by the two complementary Ti_xO_y buildingblock representations shown in *figure 2* [33, 34].

Rutile TiO_2 has a tetragonal structure and contains six atoms per unit cell. Titanium cations are surrounded by a slightly distorted octahedron of 6 oxygen atoms. Rutile is the thermodynamically most stable phase and has the highest refractive index at visible wavelengths of any known crystal. Rutil nanoparticles are mainly used in sunscreens.

Anatase also forms tetragonal crystal system. Difference is just in the distortion of the TiO_6 octahedron which is slightly larger in anatase than in rutile. The anatase structure has higher electron mobility, low dielectric constant and lower density and because of these properties it is preferred over other polymorphs for solar cell applications. Anatase phase TiO_2 nanoparticles are also used in sunscreens, sometime in combination with rutile [23]. It is difficult to dissolve anatase and especially rutile phase, for example using aqua regia for digestion of these two phases is improper. Therefore some other acids or mixtures have to be considered. For example TiO_2 is soluble in concentrated H_2SO_4, thus sulfuric acid or mixture with it can be used.

Brookite has orthorhombic crystal system. Its unit cell is composed of eight formula units of TiO_2 and is formed by TiO_6 octahedra with edge-sharping. It is more complicated, has a larger cell volume and it has also the lowest dense of the 3 forms. Brookite transforms into rutile at quite low temperatures [34, 35].

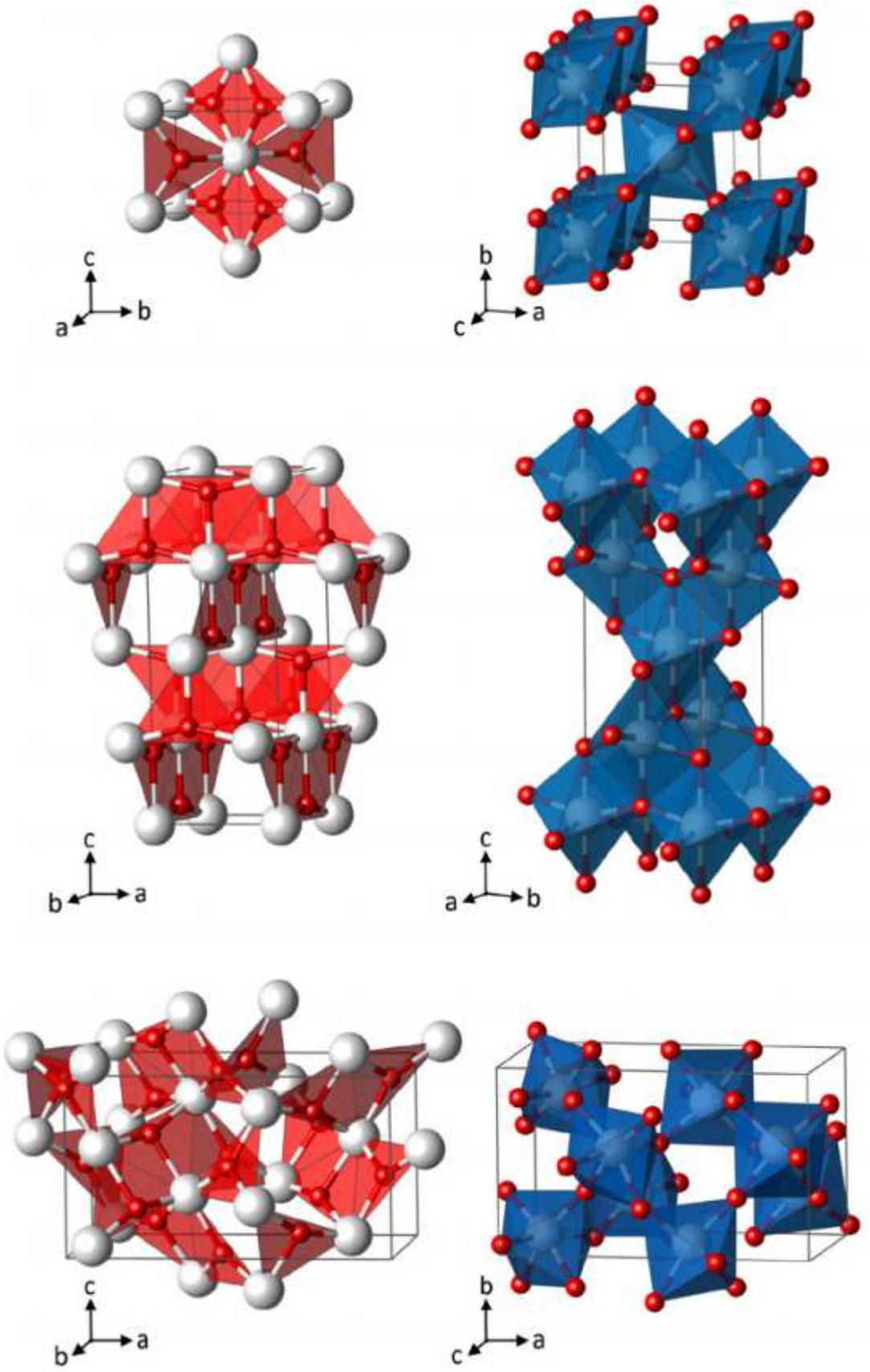

Figure 2 – planar Ti_3O *buildingblock representation* (*left side*) *and* TiO_6 *polyhedra* (*right side*) *for the rutile* (*a*), *anatase* (*b*) *and brookite* (*c*). Ti *atom – white and* O *atom – red* [33].

3.3 Nanoparticles

The nanoparticles or NPs are particles with sizes in the nanometer range. For example, the newspaper sheet is about 100 000 nm thick. Generally, particles from 1 nm to 100 nm are called nanoparticles. The term "colloid" is used for particles sizing from approximately 1 nm to 1 µm. It is important to note that there neither clear neither widely accepted definition based of physical properties for nanoparticles.

Below a given particles size some materials show different properties compare to those of the corresponding bulk material. Number of atoms and molecules located on the surface, is increasing by decreasing the particle size which leads to changes in dissolution, adsorption and reaction rate of the particles. These are the most important reasons why materials are increasingly applied in form of nanoparticles [36, 37].

According to the recommendation of European Union Commission number 2011/696/EU [6] definition of nanomaterial is: *"A natural, incidental or manufactured material containing particles, in an unbound state or as an aggregate or as an agglomerate and where, for 50 % or more of the particles in the number size distribution, one or more external dimensions is in the size range 1 – 100 nm."*

3.3.1 Properties of nanoparticles

3.3.1.1 Particle size

Particle size is the most important parameter in practical applications of powder-particles. Usually powder consists of particles of various sizes and therefore, it is necessary to characterize mean particle size and size distribution. Particles are three-dimensional objects with various shapes. Usually size of spherical particles by is described by its diameter. For particles with irregular shape it is more suitable to represent size using geometric size or equivalent size. Geometrical size can be calculated as an arithmetic mean of its width, thickness and length values, which are obtained by three-dimensional measurements. Equivalent size can be represented by operating parameters such as sieve diameter (based on sieving), Z-averaged diameter, and Stokes (or hydrodynamic) diameter (based on particle motion in fluid). All these equivalent sizes give usually different values depending on particle geometry [36].

3.3.1.2 Particle shape

Particle shape analyzers cannot be easily found unlike particle size analyzers Shape index of nanoparticles can be calculated from images of particles observed in various types of microscopes. Diameters of the NPs are usually smaller than wavelength of visible light, so nanoparticles cannot be observed by optical microscopes. Scanning electron microscope (SEM) or transmission electron microscope (TEM) must be used to get the projection images [36]. However, microscopy techniques generally produce two dimensional pictures that have to be interpreted in terms of three dimensional objects.

3.4 Analytical methods

3.4.1 Ultracentrifugation

Analytical ultracentrifugation (AUC) is a versatile and powerful method for the characterizing macromolecules and particles in solutions. Ultracentrifuge is a centrifuge optimized for spinning a rotor at very high speeds generating acceleration as high as 2 000 000 g. There are three optical systems available for the analytical ultracentrifuge - absorbance, interference and fluorescence that permit precise and selective observation of sedimentation in real time. This allows the operator to observe the evolution of the sample concentration versus the axis of rotation profile as a result of the applied centrifugal field.

There are two commonly performed types of experiments: sedimentation velocity and sedimentation equilibrium. Sedimentation velocity experiments focus on the interpretation of the entire time-course of sedimentation, and report on the shape, molar mass of the macromolecules and their size-distribution.

Sedimentation equilibrium is a thermodynamic method where equilibrium concentration gradients at lower centrifugal fields are analyzed to define molecule mass, assembly stoichiometry, association constants and solution nonideality [38, 39].

3.4.2 Ultrafiltration

Ultrafiltration (UF) is a membrane based technique. Ultrafiltration is not fundamentally different from microfiltration. Both of these separate based on size exclusion or particle capture. Main forces leading to a separation through a semipermeable membrane are pressure or concentration gradients. Suspended solids and solutes of high molecular weight are retained in the so-called retentate, while water and low molecular weight solutes pass through the membrane in the permeate. Ultrafiltration techniques (pore size of membrane below

100 nm) are widely used in chemical engineering, semiconductor, pharmaceutical, food and beverage industries and for purifying drinking water [40].

3.4.3 Chromatography

The general common character of chromatographic techniques is continual separation of compounds between stationary and mobile phase. However, the size exclusion chromatography (SEC) and hydrodynamic chromatography (HDC) are exceptions and in these cases the interactions of the analyte with the stationary phase have to be minimized. As a stationary phase is some solid or liquid substance used. The main role of mobile phase is to cause movement of components through the chromatographic system. As a mobile phase is some liquid or gas used.

Analytes are separated dependently on their different speed through the system. In liquid chromatography, speed of component is dependent on its interactions with stationary and mobile phase. Compound with stronger affinity to stationary phase is longer held on stationary phase therefore its moves slower than compound which has stronger affinity to mobile phase [41, 42]

3.4.3.1 Liquid Chromatography, HPLC

Liquid chromatography involves separation of nonvolatile, weak volatile and heat-labile compounds which represents almost 80 % of all compounds. Systems with different liquid mobile phase and solid or alternatively liquid stationary phase are used. The main factor affecting the process of separation is character of mobile phase. Choosing suitable solvent or mixture of solvents with suitable polarity, pH, etc. dependently on separated compounds is the most important step of whole separation process.

In high-performance liquid chromatography (HPLC) columns with suitable stationary phase by very small particles (3 – 10 μm) are used to achieve fast and high resolution separation. By using homogenous column filling with narrow distribution of very small particles decrease of undesirable edge diffusion, molecular diffusion in the liquid and the acceleration of the mass transfer between the phases can be achieved. Finally it results in greater efficiency chromatographic systems. The arrangement of HPLC system is shown in *fig. 3*. HPLC is not commonly used for determination of particle size, however SEC and HDC are employed in this case [41, 42, 43].

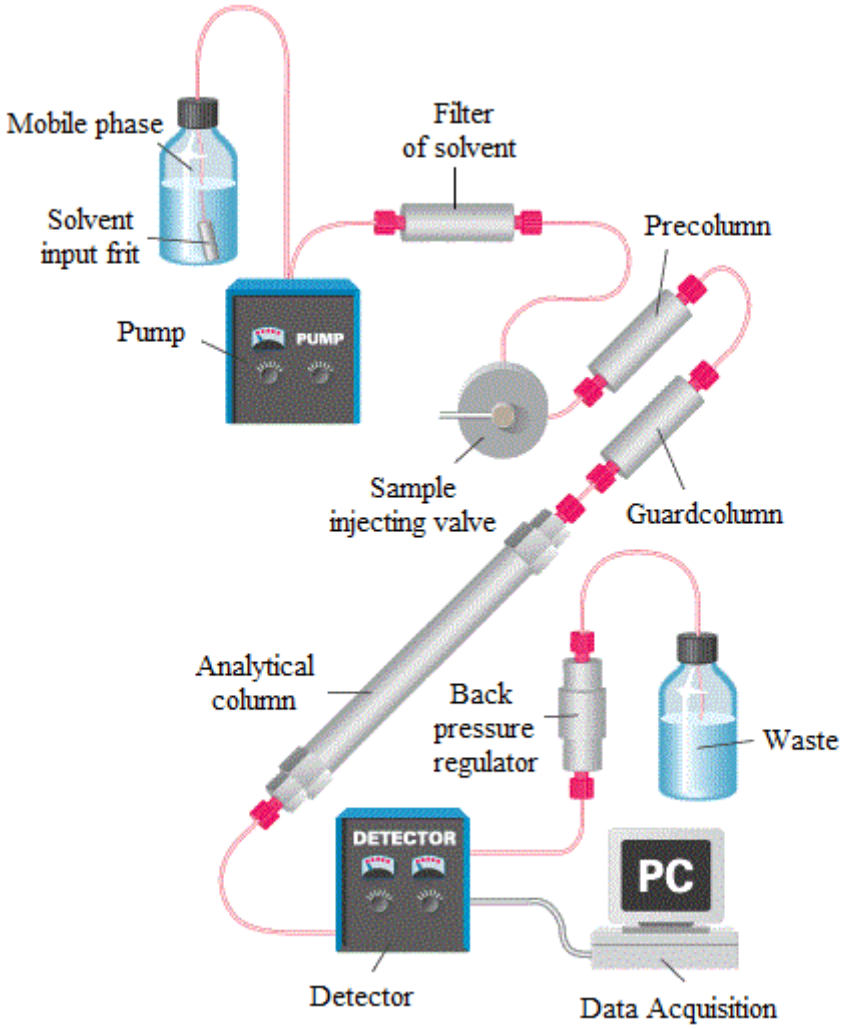

Figure 3 – example on an of HPLC set-up [44].

3.4.3.2 Size exclusion chromatography

While several examples of the use of HPLC for nanoparticle separation have been reported [45, 46], size exclusion chromatography, is one of the most popular chromatographic techniques used to fractionate NPs.

SEC is based on the differences in the particles hydrodynamic volumes and not on the interaction of these particles with the stationary phase. Small particles travel freely through the pores of the stationary phase and thus travel through the column slowly. Opposite, large particles which do not may get inside the pores of the stationary phase can travel only through the accessible volume and it means they elute more rapidly.

SEC has been used in the separations of different types of NPs including gold, silica, and semiconductor ones [47]. For successful resolution of a mixture by SEC, is necessary to choose proper eluent and stationary phase.

3.4.3.3 Hydrodynamic chromatography

Hydrodynamic chromatography HDC is also one of the techniques for particle size determination in the micro or nano range. It has some similarities with size exclusion chromatography. For example components are eluted in the order of decreasing size, as in SEC [48].

HDC system has principally the same arrangement like HPLC. The main difference is that in HDC columns packed with nonporous beads are used. Laminar flow of an eluent in column leads to creation of parabolic velocity profile with the highest velocity is in the center of the tube. For geometric reasons larger particles are statistically located preferentially close to the axis of the capillary, whereas smaller particles are located preferentially close to the walls. Behavior difference of particles with different sizes in the flow is one of the most important separation mechanisms [48, 49].

The main advantages of hydrodynamic chromatography are that it is a rapid and convenient method for the separation of particles the separation and simple operation of equipment. Disadvantages are low resolution, HDC also require correction for peak dispersion and calibration for signal intensity according to size, which however can be minimized by using ICP-MS as a detector [48].

Possibility of HDC columns to separate particles in the range 5 – 3 000 nm [], rapid analysis time and minimal requirement for sample pretreatment in combination with the features of ICP-MS measurements like selectivity and sensitivity make HDC-ICP-MS a powerful and promising technique for investigating the fate of a significant range of NP types.

Hydrodynamic chromatography coupled online with inductively coupled plasma with mass spectrometry can be used for detecting and studying the behavior of metal-containing engineered NP in complex environmental matrixes. HDC-ICP-MS was already used for example to measure the Ag NPs sizes in surface and wastewater samples [50] or for ultratrace detection of metal-containing nanoparticles [51].

3.4.4 Light scattering techniques

When light hits a small object (a particle or a molecule) it changes its direction. This phenomenon is called light scattering and it is used in light scattering techniques.

Light scattering is one of the most commonly-used techniques for measuring the particle size, the most important physical property of NPs. Instead of measuring particle size directly, specific parameters affected by particle size are measured. Examples of these parameters

include the particle's settling velocity, the volume of a medium that the particle displaces, and the pattern produced by scattered light [52, 53].

Light scattering can be divided into two methods [53]:

- **Dynamic light scattering (DLS)**
- **Static light scattering (SLS)**

3.4.4.1 Dynamic Light Scattering

Dynamic Light Scattering (DLS) or it can be also called photon correlation spectroscopy (PCS) and quasi-elastic light scattering (QELS), is one of the most popular light scattering techniques. Due to possibility of particle sizing down to 1 nm diameter it is typically used for emulsions, micelles, polymers, proteins and nanoparticles or colloids as well.

In basic principle, the sample is illuminated by a laser beam which is being scattered by particles or molecules in the sample. Fluctuations of the scattered light are detected by fast photon detector at a known scattering angle θ. From a microscopic point of view the particles cause scattering of the light thereby the scattered light carry imprint of information about particle motion.

DLS measurement provides us the hydrodynamic particle size, which is defined as the size of a hypothetical hard sphere that diffuses in the same fashion as that of the particle being measured [54]. While dispersed particle moves through a liquid medium a thin electric dipole layer of the solvent adheres to its surface. This layer influences the movement of the particle in the medium. Thus the hydrodynamic diameter gives us information of the inorganic core along with any coating material and the solvent layer attached to the particle as it moves under the influence of Brownian motion. Agglomerated particles move coupled in the medium, therefore the size in this case will be determined as hydrodynamic diameter of whole agglomerate. The hydrodynamic size of a particle is calculated (1) from the translational diffusion coefficient D by using the Stokes-Einstein equation [55]:

$$d_{\mathrm{H}} = \frac{kT}{3\pi\eta D} \qquad (1)$$

where d_{H} represents hydrodynamic diameter, k – Boltzmann´s constant, T – absolute temperature, D – translational diffusion coefficient and η – viscosity. Schematic explanation of hydrodynamic parameter is shown in *fig. 4*.

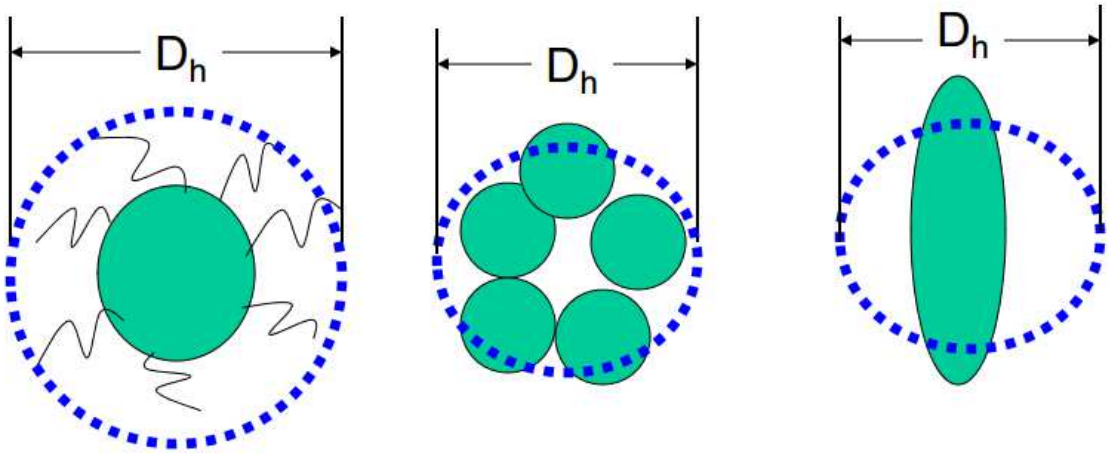

Figure 4 – schematic explanation of hydrodynamic diameter [56].

Typical arrangement of DLS instrument is shown on *fig. 5*. DLS instruments with fixed angle detector can determine the mean particle size in a limited size range. Full particle size distribution can be determined by multi-angle instruments [53, 57].

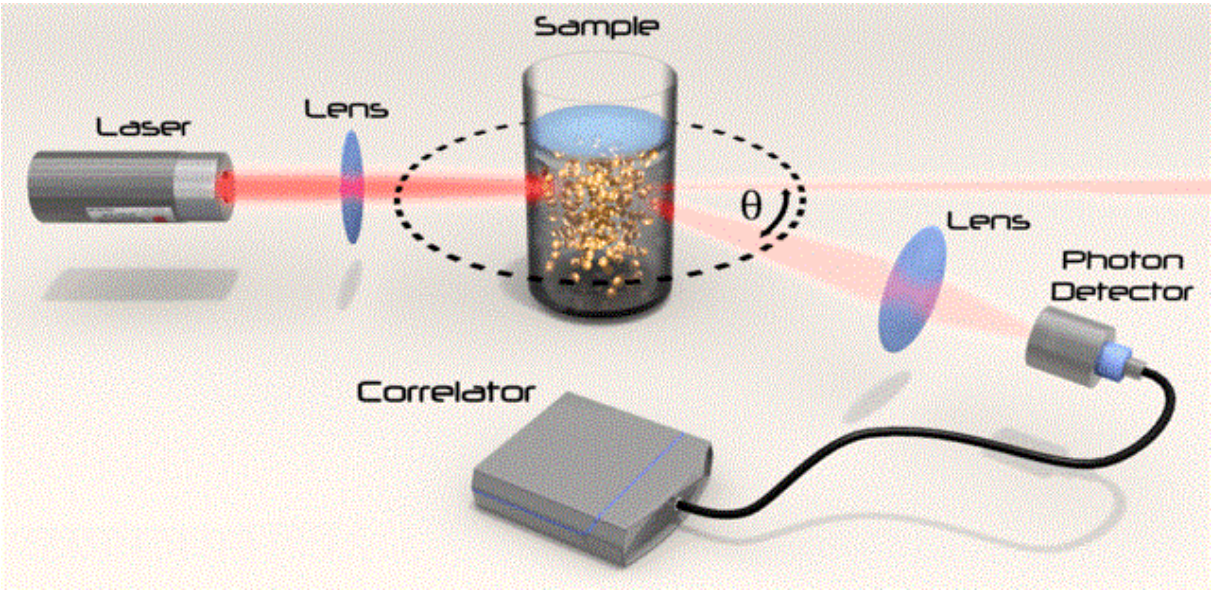

Figure 5 – set-up of a fixed angle DLS instrument [57].

3.4.4.2 Static Light Scattering

In Static Light Scattering (SLS) the intensity of the scattered light is measured in dependence of the scattering angle to obtain information on the scattering source. Typically the technique is used to determine the average molecular weight M_w of a macromolecule such as a polymer or a protein. Measurement of the scattering intensity at different angles allows calculation of the root mean square radius, also called the radius of gyration R_g. By measuring the scattering

intensity for one macromolecule at various concentrations, the second virial coefficient A_2, can be calculated.

In principle laser is used to illuminate a sample in the cuvette. Intensity of scattered light is measured in dependence of the scattered angle θ (see *figure 5*) by one or many detectors. Measured scattering curve contains information about the scattering particle size, its shape and molar mass. In case of measuring the average molecular weight, SLS instrument is calibrated using a known reference compound such as toluene. The Rayleigh ratio of toluene can be found in existing tables.

Advantage of static light scattering compare to direct imaging techniques such as SEM or TEM is that the sample can be measured in situ as long as the particle concentration is small enough to avoid multiple scattering effects and no special sample preparation is required [52, 53, 57].

3.4.5 Nanoparticle tracking analysis

Nanoparticle tracking analysis (NTA) is an emerging technique detecting simultaneously sub-micron particle, size distributions and concentrations of particles in liquid suspension. A laser beam passes through the sample chamber and the particles in suspension cause scattering of the beam. The scattered light can be easily visualized and recorded by a video camera mounted onto microscope with 20 × magnification. The charged coupled device (CCD) camera captures a video file with particle movements under Brownian motion and the video is then analyzed in NTA software, which tracks many particles individually. Using the Stokes Einstein equation software calculates hydrodynamic diameter of particles, in the same principle as in case of DLS [58, 59].

NTA technique offers the simultaneous multiparameter analysis of NPs in suspension concerning size distribution, particle concentration and direct and real-time visualization. It saves as time as sample volumes while minimal sample preparation is needed [59]. Configuration and base principle of NTA is shown in *fig. 6*.

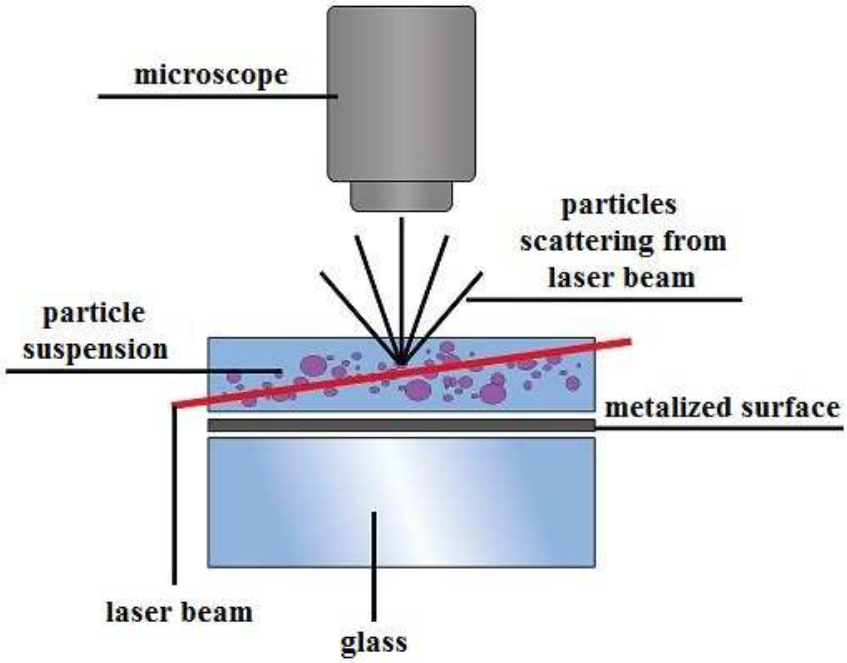

Figure 6 – schematic illustration of the optical configuration used in NTA [58].

3.4.6 Digestion

To determine total amount of titanium present in sunscreen lotion, digestion of samples is needed. Mostly in different studies it was done by microwave-assisted digestion.

In the first study [60] 150 mg of homogenized lotion and 0.5 ml of concentrated HNO_3 was added to a PTFE reactor for microwave digester, and the mixture was irradiated at 600 W for 1 min. The reactor was left to cool and than 0.5 ml of concentrated HCl was added and an irradiation for 1 min was carried out again at the same power. After one more irradiation under the same conditions the digestion product was transferred to a porcelain crucible and 0.5 g of $KHSO_4$ was added to it. The mixture was heated with a bunsen flame during a few minutes for fusion, the molten residue was dissolved in concentrated H_2SO_4 and the solution was diluted with deionized water to carry out ICP-OES analysis.

In another study [61] sunscreen was digested easier. Approximately 100 mg of sunscreen, 3 ml of $HNO_3$and 1 ml of HF were transferred into a digestion vessel. Sample was then digested at 210 °C for 20 minutes. After microwave digestion, the sample solutions were diluted to 50 ml with ultra-pure water.

Sunscreen samples can be [62] acid digested in poly-tetrafluoroethylene (PTFE) vessels. An accurately weighed portion of the sample 100-150 mg, was placed into PTFE vessel, with the 3 ml of concentrated HNO_3, 3 ml of concentrated HCl and 1 ml of HF. The vessels were closed, placed into a steel pressurized bomb and heated up to 125-130 °C for 2 h. The final digest was diluted to volume with 0.5 M HNO_3.

In next study [63] was tied hot block digestion of approximately 500 mg of lotion in concentrated HNO_3, H_2O_2 (30%), and concentrated HF. The digested samples were diluted to a total volume of 50 ml in 1% HNO_3. A 0.5 ml aliquot of this volume was diluted to 10 ml in 1 % HNO_3.

Other procedure of microwave-assisted digestion was found out [3,64]. Firstly 6 ml of HNO_3 (65%), 3 ml of concentrated HF and 1 ml of H_2O_2 (35%) were added to the sample. Then, the vessels were sealed and subjected to the following digestion program: step 1 - a 15 min linear ramp from 0 to 210 °C, and step 2 - holding the temperature at 210 °C for 10 min. Samples were cooled and then, 1.5 g of H_3BO_3 were added to each vessel to complex the residual hydrofluoric acid or dissolve precipitated fluorides salts. In this step samples were mineralized by applying the following program: l10 min linear ramp from 0 to 170 °C followed by holding the temperature at 170 °C for 10 min. The digested extracts were transferred to volumetric flasks and diluted to 100 ml with ultra-pure water.

According to low solubility of rutile and anatase phases in aqua regia, as was mentioned above and because of toxicity of HF and tediousness of fusion methods there is an effort to choose different digestion method. Rutile and anatase phases are soluble in concentrated H_2SO_4 and therefore, using concentrated H_2SO_4 and 30 % H_2O_2 as strong oxidizing agent can be considered for digestion of sunscreen lotion.

3.4.7 ICP-MS

Inductively coupled plasma mass spectrometry or ICP-MS is an analytical technique used for ultra-trace elemental analysis. From 1983, when the technique was commercially introduced it was extended in many types of laboratories where very high sensitivity analyses are required. ICP-MS has many advantages over other elemental analysis techniques [65]:

- detection limits for most elements even better than those obtained by Graphite Furnace Atomic Absorption Spectroscopy (GFAAS)
- higher throughput than GFAAS
- the ability to handle both simple and complex matrices with a minimum of matrix interferences due to the high-temperature of the ICP source
- superior detection capability to ICP-OES with the same sample throughput
- the ability to obtain isotopic ratio

The principle of ICP-MS is a combination of a high-temperature inductively coupled plasma (ICP) source with a mass spectrometer (MS). Firstly, atoms of the elements in the sample are converted to ions in the ICP source then these ions are separated and detected by the mass spectrometer [66].

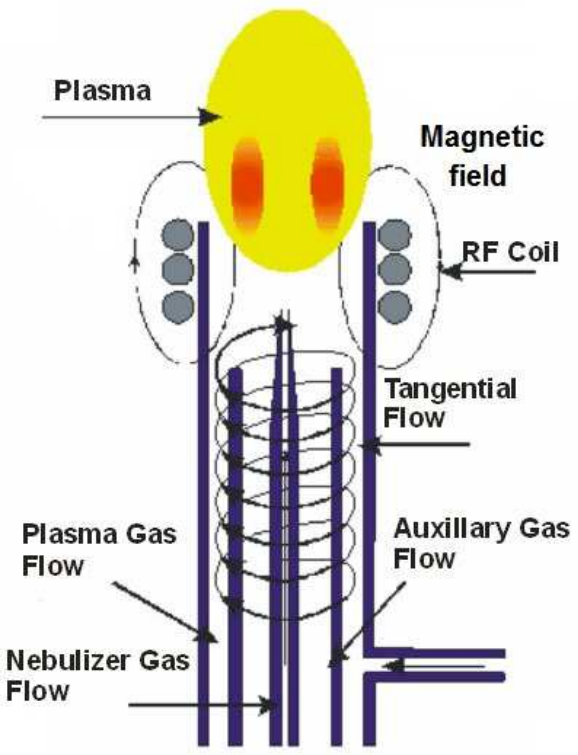

Figure 7 – ICP source [67].

Fig. 7 shows a schematic representation of an ICP source. The nebulized sample is carried in the flow of plasma support gas, which is typically Ar. The plasma torch consists of concentric quartz tubes. The inner tube contains the sample aerosol and Ar support gas and the outer tube contains flowing gas to keep the tubes cool. A radio frequency (RF) generator (typically 1-5 kW) produces an oscillating current in an induction coil that wraps around the tubes which leads to induction an oscillating magnetic field. When a spark is applied to the argon gas flowing through the ICP torch, electrons are stripped off of the argon atoms, forming argon ions. These ions are caught in the oscillating fields and collide with other argon atoms, forming an argon discharge or plasma [65, 67].

Nebulized sample from nebulizer are carried to the formed plasma, with a temperature of around 6 000 – 10 000 K. Elements in the sample after converting into ions, typically positive ions M^+ or M^{2+},are then brought into the mass spectrometer via the interface cones. Analysis of the content of the various ions in the sample can be carried out only under conditions of relatively high vacuum, it is necessary to transport the argon sample stream at atmospheric

pressure (1-2 Torr) into the low pressure region. This is accomplished by passing a sample of two cones with a diameter of the inlet port a few tenths of a millimeter. After passing through the first cone (sampler), the ions of the sample get into the space where the pressure is in the order of 10^{-2} Torr. After passing through a second cone (skimmer) analyzed sample gets into the environment at a pressure approximately 10^{-5} Torr.

The formed ions are then guided by the system of electromagnetic lenses towards the analyzer, where they are separated by their mass-to-charge ratio (m/z). Only ions with the selected mass go on the detector. Impact of analyzed ions on the surface of the amplifier of the detector induces a very weak electrical current, which is then amplified and its intensity is measured [65, 66].

Types of MS analyzers used in ICP-MS tandem [66]:

- **Quadrupole mass filter** – the most commonly used
- **Time of flight (TOF)** – still experimental but highly promising
- **Combination of electric and magnetic sector** – high resolution MS - high demands on vacuum and price but completely eliminating spectral interference

In *fig. 8* is shown example of arrangement of ICP-MS equipment with quadrupole analyzer.

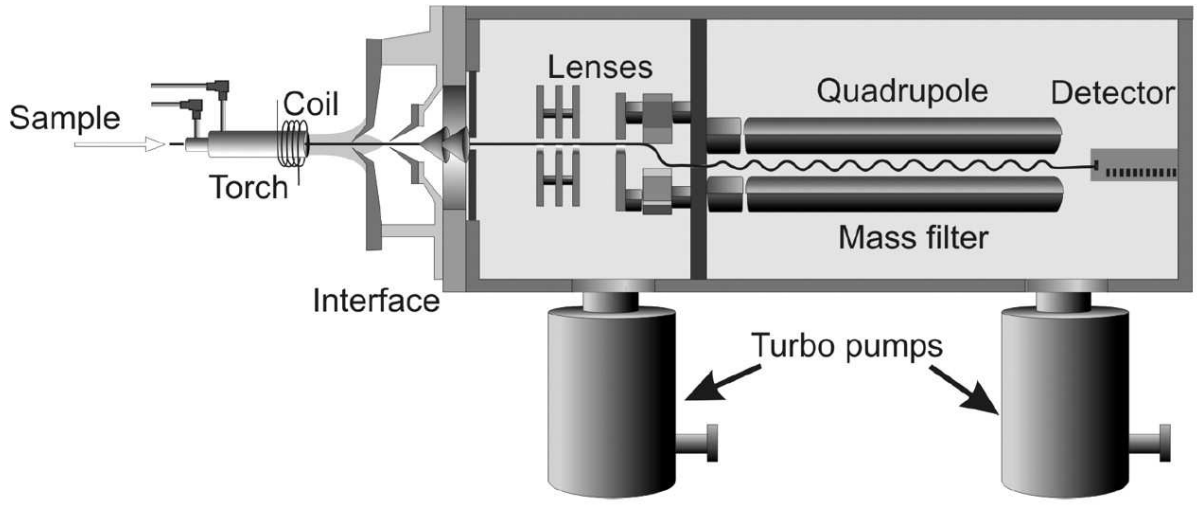

Figure 8 – example of arrangement of ICP-MS equipment [67].

3.4.8 ICP-OES

Inductively coupled plasma optical emission spectrometry or ICP-OES is an analytical technique used for the detection of trace metals. The first step is principally the same with ICP-MS. Inductively coupled plasma is used to excite atoms and ions which emit electromagnetic radiation. Liquid and gas samples may be injected directly into the instrument, while in case of solid samples extraction or acid digestion is required.

The sample solution is converted to an aerosol and directed into the central channel of the plasma which was explained above. Sample is quickly vaporized and analyte elements are liberated as free atoms in the gaseous state. In plasma sufficient energy is often available to convert the atoms to ions and subsequently excite the ions.

Excited state species may then relax to the ground state via the emission of a photon. These photons have characteristic energies thus the wavelength of the photons can be used to identify the elements from which they originated. The intensity of emission is directly proportional to the concentration of element in the sample.

The ICP-OES instrumentation is relatively simple. A portion of the photons emitted by the ICP is collected with a lens or a concave mirror. This focusing optic forms an image of the ICP on the entrance aperture of a wavelength selection device such as a monochromator. The particular wavelength is converted to an electrical signal by a photodetector. The signal is amplified and processed by the detector electronics, then displayed and stored by a personal computer [68].

3.5 Electron microscopy

In electron microscope (EM) is beam of electron used to create an image of specimen. To compare with light microscope, electron microscope has much higher magnification and greater resolving power. A modern light microscope, by comparison, has a magnification of about 1000 times and enables the eye to resolve objects separated by 200 nm. Light microscopes are limited by wavelength of the light.

Electron microscope consists of four main components: an electron optical column, a vacuum system, the necessary electronics (lens supplies and high voltage generator) and control software. The electron column includes elements analogous to those used in a light microscope. Instead of light source is used electron gun, and glass lenses are replaced by electromagnetic lenses in electron microscope.

All electron microscopes use electromagnetic and (or) electrostatic lenses to control the path of electrons. The electron beam passes through the center of such solenoids on its way down the column of the electron microscope towards the sample. Electrons due to their sensitivity to magnetic fields can be controlled by changing the current through the lenses. The more accelerated the electrons are, the shorter their wavelength will be. The resolving power of a microscope depends on the wavelength of the irradiation used to form an image [69,70].

There are two base types of electron microscopes:

- **Transmission Electron Microscope (TEM)**
- **Scanning Electron Microscope (SEM)**

There are two base types of projection images of material which can be done [36]:

- **Two-dimensional particle projection** – as a microscopic photography
- **Three-dimensional particle projection** – taking two microscopic pictures from slightly different angles leading to 3D information. It can be taken by three-dimensional scanning electron microscope (3D-SEM). More detailed shape analysis can be done by TEM-CT which is similar to computer aided tomography and it can take 120 transmission images when sample is rotated form – 60 to + 60 degrees with step one degree.

3.5.1 Transmission electron microscopy

TEM uses high voltage electron beam emitted by a cathode and formed by magnetic lenses which passes through a thin specimen. Partially transmitted electrons from very thin specimen are collected, focused, and projected onto the viewing device at the bottom of the column. This transmitted electron beam carries information about the structure of the specimen. The entire electron path from electron gun to camera must be under vacuum. The spatial variation in this information (the "image") is magnified by a series of magnetic lenses until it is recorded by hitting a fluorescent screen, photographic plate, or light sensitive sensor such as a charge-coupled device (CCD) camera. The TEM may provide in real time displaying of the image detected by the CCD on a monitor or computer.

Transmission electron microscopes produce two-dimensional, black and white images. Spherical and chromatic aberration cause limitations of the resolution of the TEM, but it can be partially corrected by new generation of aberration correctors. Software correction of spherical aberration allows the production of images with sufficient resolution to show carbon atoms in diamond separated by only 0.089 nm at magnifications of 50 million times. The TEM is an indispensable tool for nano-technologies research and development in many fields thanks its atomic resolution. In the life sciences, the resolution is still mainly limited by specimen preparation not by microscope [69, 70].

3.5.2 Scanning electron microscope

In contrast with the TEM, where the electrons in the primary beam are just transmitted through the specimen, the scanning electron microscope produces images by detecting

secondary electrons which are emitted from the surface due to excitation by the primary electron beam. The electron gun at the top of the column produces an electron beam that is focused into a fine spot (as small as 1 nm in diameter) on the specimen surface. This beam is scanned in a rectangular raster over the specimen with detectors building up an image by mapping the detected signals with beam position and data stored in computer memory.
There are some advantages of the SEM in comparison to TEM:

- SEM uses beam focused to fine point and scans line by line over the sample surface in rectangular raster pattern
- The accelerating voltages are much lower than in TEM due to no necessity to pass through the specimen
- The specimen does not need to be thin, which greatly simplifying its preparation

Although SEM resolution is about an order of magnitude lower than the TEM resolution, the SEM is able to image bulk samples and has a much greater depth of view because the SEM image relies on electron interactions at the surface rather than transmission. So it can produce images that are able to represent the 3D structure of the sample. Therefore, it is considered that SEM images provide us with 3D, topographical information about the sample surface [69, 70, 71].

3.5.2.1 The most common detectors in SEM

The electrons of the primary beam interact with atoms in the sample, producing various signals (*figure 9*) that contain information about the surface topography and composition of the sample. These signals can be detected [72].

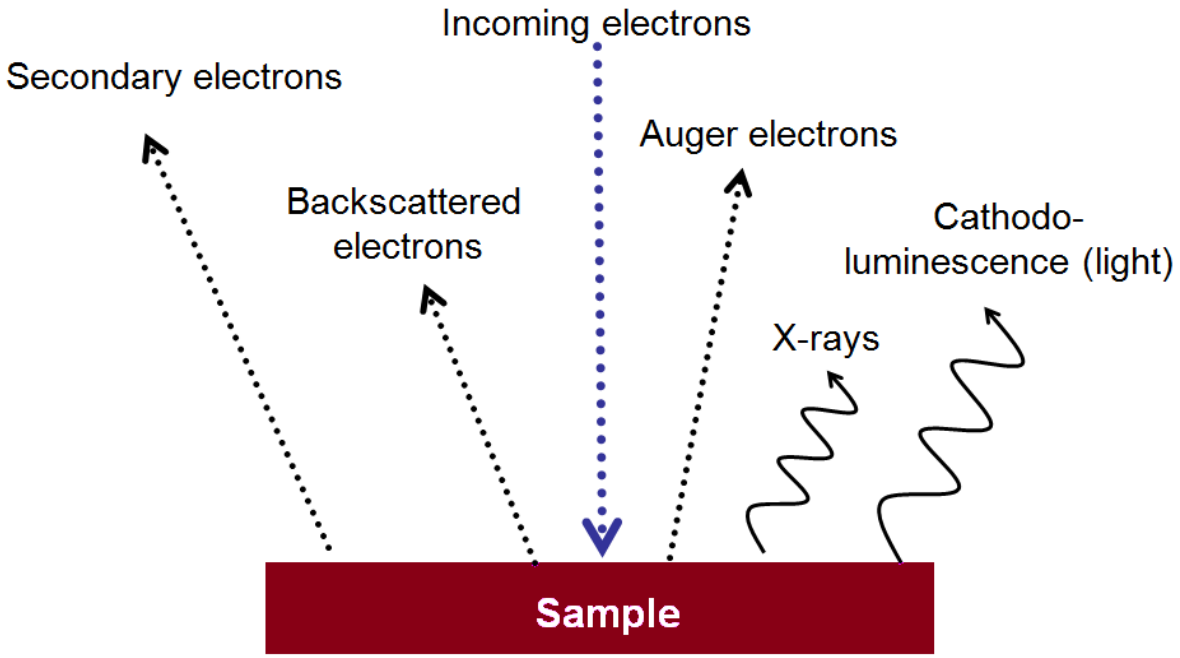

Figure 9 – present signals after primary beam electrons interaction with sample [72].

Everhart-Thornley Detector (ETD)

The Everhart-Thornley detector uses the secondary electron signal to formation of images, The end result is higher potential resolution using this signal. Typically it consists of a Faraday cage, scintillator coupled to a light pipe and photomultiplier tube.

The Faraday cage, which is typically kept at a positive potential, is efficiently collecting most of the secondary electrons (less than 50 eV) emitted from the sample. Incoming electrons are accelerated by the scintillator with a high positive charge and they can be converted to light photons there. The photomultiplier produces an output signal that is then related to the total number of electrons collected [72,73].

Back Scattered Electron Detector (BSED)

The BSED is mounted below the objective lens pole piece and centered around the optic axis. Backscattered electrons are generated as the specimen surface is scanned by the primary electron beam electrons. Backscattered electrons carry the topographical, physical and chemical characteristics of the sample. Both compositional and topographical backscattered electron images can be detected depending on the window of electron energies selected for image formation [74].

Sample Current Detector

A sample current detector is a very sensitive ammeter with a fast response time that measures the current passing from the sample stage to ground. Total current is a function of the backscattered, secondary and auger electron yield at any point on the sample. This signal is

sensitive to all the contrast mechanisms of the other electron signals. Backscattered and secondary electron signals are dominant to this signal, and because the secondary yield is in dependent on the backscattered yield, the sample current signal typically resembles the inverted backscattered electron signal [72].

Cathodoluminescence (CL)

As sample surface is scanned by electron beam, optical photons are emitted by some excitated materials. A cathodoluminescence detector is sensitive to these optical photons. The detector typically consists of mirrors and light guides and a photomultiplier tube [72].

X-RayDetectors

X-ray detectors examine the X-ray spectrum emitted by the sample under the influence of the primary beam electrons. Because most elements emit easily measurable characteristic X-rays, the X-ray spectrum collected from each region of a sample can provide useful information on the elemental composition of the region of the sample under the electron beam [75].

Energy Dispersive Spectroscopy Detector (EDS or EDX)

Energy Dispersive Spectroscopy or Energy Dispersive X-ray Detector is essentially a large single crystal semiconductor that absorbs the energy of incoming X-rays by ionization, yielding free electrons in the crystal that become conductive and produce an electrical charge bias. The X-ray absorption thus converts the energy of individual X-rays into electrical voltages of proportional size. The electrical pulses correspond to the characteristic X-rays of the element. A computer keeps track of the number of counts within each energy range, and the total collected X-ray spectrum can then be determined [72, 75].

Wavelength Dispersive X-Ray Detector (WDS)

A WDS detector uses X-ray diffraction to separate the different X-ray energies emitted from the sample. Compare to EDS detector, WDS tend to require much more space, as well as higher probe currents and long collection times. That leads to much higher resolution than EDS and it making the detector of choice for samples with many closely spaced peaks, or careful analytical work [72].

3.5.3 Sample preparation

In general, materials to be viewed in an electron microscope require preparation to create a suitable sample. Preparation has to be done because of high vacuum inside of an electron microscope. The preparation technique required depends on the specimen, the analysis required and the type of microscope. There exist several preparation techniques [69, 76]:

Cryofixation - rapid freezing of the specimen (typically to liquid nitrogen temperatures) which causes that specimen is preserved in snapshot of its solution state.

Fixation - process of preserving a sample at a moment in time to prevent further deterioration, so that it appears as close as possible to what it would be like in the living state, although it is now dead. For electron microscopy, glutaraldehyde is often used to crosslink protein molecules and osmium tetroxide to preserve lipids.

Dehydration - process of replacement of water in the sample with organic solvents (ethanol or acetone ect.) and total drying for SEM specimens or infiltration with resin and subsequent embedding for TEM specimens.

Embedding - tissue infiltration with resin, which leads to create a hardened block by polymerization followed by sectioning.

Sectioning - the production of very thin slices of the specimen, which must be semitransparent to electrons (around 90 nm). Glass or diamond knifes are used for sectioning of material on ultramicrotone.

Staining - samples are stained by heavy metals (lead or uranium) to increase electron density leading to higher number of interactions between the electrons in the primary beam and those of the sample, which gives us contrast between different structures. Suitable for materials that are nearly “transparent” for electron beam.

Freeze-fracture and **freeze-etch** - the fresh tissue or cell suspension is cryofixed, and then fractured. The cold, fractured surface is generally "etched" by increasing the temperature to about - 95 °C for a few minutes to let some surface ice sublime to reveal microscopic details. The sample is now ready for imaging by SEM. For the TEM, it can then be rotary-shadowed with evaporated platinum at low angle in a high vacuum evaporator. A second coat of carbon, evaporated perpendicular to the average surface plane is generally performed to improve stability of the replica coating. After returning the specimen to the room temperature and pressure, can be extremely fragile "shadowed" metal replica of the fracture surface released from the biological material. It is usually by careful chemical digestion (acids, hypochlorite solution or SDS detergent can be used). The metal replica is after washing from residual chemicals viewed in the TEM.

Sputter Coating-to prevent charging of the specimen which would occur due to accumulation of static electric fields during imaging is sample coated with an ultra-thin layer of electrically-conducting material (gold, gold/palladium, platinum, chromium etc.). The amount of secondary electrons is increased too, therefore signal to noise ratio is higher in SEM.

3.5.4 TiO_2 nanoparticles

TiO_2 nanoparticles are manufactured worldwide in large quantities for use in a wide range of applications. They have been used in industrial and consumer products due to their stronger catalytic activity compared with fine particles (FNs) analogs. TiO_2 NPs possess different also other physicochemical properties compared to their fine particle of TiO_2, which might alter their bioactivity.

Although TiO_2FPs have been considered as poorly soluble, low toxicity particles for a long time, recently, TiO_2 particles were classified as a Group 2B carcinogen (possibly carcinogenic to humans) by The International Agency for Research on Cancer (IARC) because of developed lungs tumors in rats after two years of exposure to high concentrations of fine TiO_2 particles. In the case of sunscreens the most probable exposure would be dermal absorption, cause of direct applications of lotions on the skin [77].

Based on sufficient evidence using experimental animals, titanium dioxide was reclassified from unclassifiable as to carcinogenicity in humans (group 3 - carcinogen) to possibly carcinogenic to humans (group 2B - carcinogen) in 2006 [78].

According experimental investigation of NP penetration through skin, TiO_2 nanoparticles in sunscreens, even after multiple successive applications during four days, were located mainly the uppermost part (1 - 2 μm from the surface) of the outermost layer of the epidermis [79].

Other study of NPs penetration showed similar results. 90 % of 20 nm TiO_2 component of sunscreens was found within the first 15 tape strips after 5 h after emulsion application. Study confirms that TiO_2 accumulates in the uppermost layers of the epidermis. No TiO_2 was detected in the viable skin layers through either transcorneal or transfollicular pathways [80].

Except the effect of light absorption or scattering, TiO_2 particles also provide interaction, in biological tissues [81]. Free radical generation was obtained in presence of semiconductor particles upon UV irradiation. The absorption of UV photons can leads to free radical formation. Free radicals not only destroy the sunscreen base, but they are also harmful for living cells. Large quantities of free radicals can provoke cancer, the situation which sunscreens should prevent from. Recent studies have shown that the toxic effects of TiO_2 particles are dose and size dependent. For example, 20 nm TiO_2 NPs are photo active on the human skin, producing free radicals that might damage supercoiled skin cell DNA, even at low doses and in the absence of exposure to UV [82, 83]. Therefore, light absorbing particles should be handled with caution. Modern sunscreens, however, contain beta-carotene and lycopene that reduce this negative effect [77].

Now, NPs have entered a period of commercial exploitation there is growing interest in developing techniques able to characterize particles size, especially in view of the evidence that the chemical and toxicological properties of NPs are size-dependent.

3.5.5 Fate of TiO_2 nanoparticles in the environment

Several studies have shown that TiO_2 NPs do not penetrate the skin to any great extent and they are relatively easily removed from the skin during washing. This is how they enter seawater or wastewater streams [79, 80, 84].

A significant release of colloidal residues containing TiO_2 NPs from commercialized sunscreens into aquatic environment was obtained and it could lead to potential ecotoxicity of these residues to aquatic organisms. Stable bio-accessible dispersion of nanoparticles was generated in water [85].

Most of TiO_2 nano particles will adsorb on the sludge during waste water treatment plant [84]. Just small amounts can be found in the effluent. So, after sewage sludge applications on fields, they can enter also terrestrial environment. This is one the reason why sludge from wastewater treatment plant should not be used as a fertilizer product. Better way of treating sludge, form this point of view is incineration or disposal as landfill [84].

In case of plants, although high metal concentrations have been detected in the roots exposed to alterTiO_2NPs, no biological effect was observed [86]. TiO_2 nanoparticles are minimally water-soluble and their potential carcinogenic effects should not be attributed to the release of titanium ions in the medium. Several studies showed no mutagenicity [86, 87] or very weak mutagenicity [88] caused by TiO_2 nanoparticles in the bacterial reverse mutation test.

There is increasing need for a complete nanotechnology risk assessment to evaluate the potential fate and indirect exposure of nanocomposite-based products not only during their manufacturing or use, but also throughout their entire life cycle [85].

3.5.6 Extraction and characterization of nanoparticles in biological or commercial samples: state of the art

Based on literature research (*table 2*) the main issue in case of sunscreen samples is to extract the nanoparticles from the organic matrix. This can be achieved by using chloroform, surfactant solution or hexane for defatting the lotion first, followed by separating the particulate fraction by ultrafiltration or ultracentrifugation, for instance. This purification step should be repeated until the required purity of the obtained nanoparticle suspension is achieved.

Table 2 – extraction procedures for metal nanoparticles based on literature research.

NPs	Matrix	Extraction Procedure	Analysis	Ref.
Ag	tissue - oligochaete *L. variegatus*	1.0 g of frozen tissue was added to 10 ml of deionized water and sonicated for 1 h and then centrifuged to remove biological debris. The supernatant was analyzed.	FFF-ICP-MS	[89]
Au	tissue- rat liver	BSA was added at approximately 10-fold excess by mass relative to the gold content to 2 ml of rat liver homogenate. TMAH was then added to a final concentration of 5% (v/v). The samples were ultrasonicated for 1 h and rotated mechanically at room temperature overnight.	AFFFF-MALS/ DLS-ICP-MS	[90]
Au Ag	tissues – beef, *L. variegatus*, *D. magna*	To portion of 0.5 g (1.75 mg in case of *D. magna*) tissue 10 ml of 20% TMAH solution was added. Tissue samples were then bath sonicated for 1 h. Digested samples were diluted a minimum of 1:20	SP-ICP-MS	[91] [92]
Au Ag Pt	tissue - *D. magna*	One exposed *D. magna* per exposure experiment was directly treatedwith0.5 ml trypsin solution (trypsin re-suspended with the secondary trypsin buffer) by vortexing for around5 min. Suspension was placed in the drying cabine at 40 °C for2-4 h, After dry the Afterwards sample vials were shaken several times by hand and analyzed.	AFFFF-ICP-MS	[92]
Au	tomato roots	The roots were washed with DI water, cut into small pieces and homogenized by a hand-held tissue homogenizer in 8 ml of 2 mM citrate buffer (pH 3.5-7.0).Then 2 ml of the enzyme solution (1 g of macerozyme R-10 powder in 20 ml of ultrapure water) was added. The samples were shaken at 37 °C for 24 h. Samples were settled for approximately 1 h and 0.1 ml of the supernatant was diluted 100 times using ultrapure water.	SP-ICP-MS	[8]
Ag	chicken meat	1 g of meat paste was transferred into a 13 ml polypropylene tube and 1 ml of AgNP suspension was added to obtain a sample with a concentration of Ag NPs of 0.01% (m/m). The sample was vortex-mixed for 1 min at 2 500 rpm and subsequently 2 ml of 0.5 mM NH_4CO_3 buffer was added. The samples were centrifuged and volume of 0.5 ml of the supernatant was removed and 2 ml of the 0.5 mM NH_4CO_3 buffer was added. The diluted supernatant was passed through syringe filters with a pore size of 0.45 μm and analyzed.	AFFFF-ICP-MS	[93]

Ag	soil	Deionized water equivalent to 2.5 the moisture content of the soil was added to a soil sample to obtain a saturated phase. The saturated phase was added to a 20 ml syringe plugged with premoistened borosilicate glass wool. The syringe was suspended from the top of a 50 ml centrifuge tube and centrifuged 8 min at 1 000 rpm. Porewater extracts were filtered with 30 mm, 1.0 µm borosilicate glass fiber syringe filters prior to analysis.	AFFFF-ICP-MS	[94]
TiO_2	sunscreen	0.1 g of lotion was dispersed in 20 ml of deionized water and tip sonicated. Then 20 ml of methanol was added and suspension was tip sonicated again. After transferring the suspension to separation funnel, 10 ml of hexane was added to it and shaken for 1 min. Organic phase was separated and water/methanol phase was analyzed.	FFFF-ICP-OES	[3]
TiO_2	sunscreen, food	10 ml of hexane to 0.1 g of sunscreen lotion. Suspensions were sonicated for 5 min and centrifuged at 3000 rpm for 5 min. The hexane supernatant was removed and 20 ml of deionized water was added to the solid white residue to resuspended pelletized material. This mixture was sonicated for 30 min and subsequently centrifuged for 30 min at 3000 rpm. The supernatant water portion was analyzed. Optionally a further 0.5 ml of hexane was added after removal of the hexane used for defatting to aid particle disaggregation.	FFF-ICP-MS	[63] [95] [64]
TiO_2 ZnO	sunscreen	5 g of the sunscreen emulsion extracted with 30 ml chloroform followed by centrifugation at 4500 rpm for 15 min. This operation was repeated three times to get solid particle powder which can be easily dissolved in water and analyzed.	EDS, XRD	[96]

4. THE AIM OF WORK

In the frame of the research project InterNano [97], the fate and effects of nanoparticles on the environment have to be investigated. InterNano project focus on mobility, aging and functioning of engineered inorganic nanoparticles at the aquatic-terrestrial interface. The objective of the research unit is to identify the processes relevant for the fate of engineered inorganic nanoparicles and pollutants associated with it in the interfacial zone between aquatic and terrestrial ecosystems [97].

TiO_2 nanoparticles are presented in an increasing number of commercially available products and it carries also increasing need to evaluate the potential fate and indirect exposure of TiO_2 NPs of different sizes and shapes and investigate their entire life cycle. Thus, the first aim of this work is to investigate feasibility of extracting of TiO_2 from sunscreen samples to have them in state close to a realistic release scenario. Extracted nanoparticles could be subsequently used to investigate their fate in the environment and for ecotoxicological studies. However, such experiments require an accurate knowledge of the suspension parameters. Therefore, the second part of the work aimed at characterizing extracted particles by determining average size, shape, concentration, and stability in the extraction medium.

5. EXPERIMENTAL PART

5.1 Used laboratory equipment

- equipment for ultrapure water, Reinstwassersystem EASYpure II™, Werner, Germany
- AX105 Delta Range analytical balance, Mettler Toledo, Germnay
- ultrasonic cleaner, VWR, USA
- centrifuge universal 320, Hettich Zentrifugen, Germany
- WX Ultra Series Centrifuge, Thermo Scientific, Germany
- Delsa™Nano C Particle Analyser, Beckman Coulter, Fullerton, USA
- Quanta 250 Scanning Electron Microscope, FEI, USA
- Leo 912 OMEGA Transmission Electron Microscope, Carl Zeiss, Germany
- 3 mm copper grid covered with a combined holey and ultrathin carbon film, Ted Pella, Inc., Redding, USA
- NanoSight LM20 system, NanoSight, Amesbury, United Kingdom
    - sample chamber BD Discardid II, New Jersey, USA
- Agilent 1 200 HPLC system, Agilent, Germany
    - PL-PSDA type 1 column (20-1 200 nm), Agilent, Germany
- X SERIES 2 ICP-MS, Thermo Scientific, Germany
    - PTFE spray chamber
    - platinum sample cone
    - Peltier cooler
    - quadrupole analyzer, Thermo Scientific, Germany
- Amicon Ultra-15 CentrifugalFilter Tubes, Millipore, Merck, Germany
- ordinary laboratory equipment

5.2 Used software

- Microsoft Office Word 2007, Microsoft, USA
- Microsoft Office Excel 2007, Microsoft, USA
- Paint ver. 6.1, Microsoft, USA
- PlasmaLab, Thermo, Germany
- NTA 2.0 Build 127 software
- ImageJ 1.49v, National Institutes of Health, USA

5.3 Chemicals, standards and samples

5.3.1 Chemicals

- Ultrapure water with resistivity 18.2 MΩ·cm (25 °C) was produced by Reinstwassersystem EASYpure II™, Werner, Germany
- Sulfuric acid 95 %, ROTIPURAN®, Carl Roth, Germany
- Hydrogen peroxide 30 %, ROTIPURAN®, Carl Roth, Germany
- Potassium hydroxide, flake 85 %, Alfa Aesar, Germany
- n-Hexane, ROTISOLV® HPLC, Carl Roth, Germany
- Acetone for liquid chromatography, LiChrosolv® Merck, Germany
- 2-propanol gradient grade for liquid chromatography, LiChrosolv® Merck, Germany
- Chloroform, ethanol free 99 %+, Alfa Aesar, Germany
- Sodium n-dodecyl sulfate 99 %, Alfa Aesar, Germany
- Triton X-100, Alfa Aesar, Germany

5.3.2 Standards

- TiO_2 standard P-25 nanopowder, Degussa, Braunschweig, Germany
- Citrate stabilized gold nanoparticles (spherical, diameter: 30, 50, 100, 150 and 250 nm), Sigma-Aldrich, Germany
- Single element Rh standard 1 000 ± 3 µg/ml Peak Performance, California, USA

5.3.3 Samples

Eleven commercially available sunscreen products were purchased at local shops. Sunscreens with high sun protection factor (SPF ≥ 30) were chosen for future experiments. Unfortunately, information about TiO_2 and/or ZnO content, phase composition neither size of these mineral pigments particles are not available on any of chosen sunscreens product label. Details of all sunscreen samples are shown in *Table 3*.

Sunscreens bottles were well shaken each time before taking the subsample. The first small portion of the sunscreen lotion after opening each bottle was discharged to waste and only than the subsample was taken.

Table 3 – sunscreens used for analysis.

ID	Name	Art	Additional usage	SPF	TiO_2	ZnO
01	ReweFeuchtigkeits-Sonnenspray[1)]	Lotion/spray	Sensitiv	30	yes	no
02	ReweFeuchtigkeits-Sonnencreme[1)]	Cream	For children	50	yes	no
03	Real,- Quality Sonnenmilch[1)]	Lotion	Cooling effect	30	yes	no
04	Real,- Quality Sonnencreme[1)]	Cream	Anti-aging effect	30	yes	no
05	BiothermLaitSolaire[1)]	Lotion	–	50	yes	no
06	Nivea Sun PflegendeSonnenmilch[1)]	Lotion	Cooling effect	50	yes	no
07	Sundance Sonnenmilch[1)]	Lotion	Radical Control Komplex	50	yes	no
08	Garnier Ambre SolaireResistoSonnenschutz-Milch[2)]	Lotion	For children	50	yes	no
09	Alverde Sonnencreme Jojoba[2)]	Cream	Sensitiv	30	yes	no
10	BabyloveSonnencreme[2)]	Cream	For babies	50	yes	yes
11	Baby sebamedSonnenschutzlotion[2)]	Lotion	For babies	50	yes	no

1) – sunscreens suspendable in 0.1 % Triton X-100 solution.

2) – sunscreens suspendable in hexane.

5.4 Solvent screening

If any extraction method based on ultrafiltration or ultracentrifugation is considered, it is necessary to find some suitable solvent which is able to completely suspend the sunscreen lotion. 1 % solutions of sodium dodecyl sulfate (SDS), Brij L35 and Triton X-100 surfactants were tested to investigate the ability to suspend each of the sunscreen samples. When ultrafiltration was used as separation technique, the concentration of Triton X-100 solution was chosen to be 0.1 % in order to avoid membrane damages observed when using 1 % solution with Ultra-15 Centrifugal Filter Tubes.

For samples which could not to be suspended with any of surfactants (samples number 08, 09, 10, 11) organic solvent had to be considered. Acetone, isopropanol, tetrahydrofuran, and hexane and chloroform certainly based on studies before (see *Table 2*) were tested.

Also effective solution for suspending the residue after centrifugation or ultrafiltration had to be tested because NPs extracted from sunscreens seemed to be unstable in ultrapure water and fast agglomeration was observed when ultrapure water was used for suspending them. Therefore, ability to suspend residue after ultrafiltration and ultracentrifugation of ultrapure water, ultrapure water with pH adjusted to 2 (HCl) and 12 (NaOH) and 0.1 % solution of Triton X-100 solution without and with pH adjustments to 2 (HCl) and 12 (NaOH) were tested.

5.5 Extraction of TiO_2 nanoparticles

5.5.1 Extraction by ultrafiltration

Approximately 50 mg of homogenized sunscreen lotion was weighed and added into a glass beaker with a magnetic stir bar. 10 ml of 0.1 % Triton X-100 solution (pH = 12) was added and the beaker was placed to a magnetic stirrer and stirred for 30 min until t of an homogeneous suspension was obtained. The milky suspension was transferred to Ultra-15 Centrifugal Filter Tube and centrifuged at 4 500 r.p.m. for 30 min. Filtrate from the tube was discharged and residue that stayed on the filtration membrane was resuspendedin10 ml of 0.1 % Triton X-100solution. Suspension was centrifuged again at the same conditions. This procedure was repeated to get purified suspension of TiO_2 NPs. Residue after last centrifugation was resuspendedin10 ml of 0.1 % Triton X-100 solution (pH = 12), transferred to plastic tube, sonicated for 15 min in ultrasonic bath and used for further analysis.

In case of samples 8, 9, 10 and 11 was 10 ml of hexane used instead of Triton X-100 solution and the first centrifugation was done in ordinary glass tubes at 5 000 r.p.m. for 20 min. Hexane supernatant was entirely removed by pipet and opened tube was placed to a hood for 5 min to evaporate the residual amount of hexane from the tube. Solid residue was resuspended in 0.1 % Triton X-100 solution (pH = 12), sonicated for 15 min, transferred to Ultra-15 Centrifugal Filter Tube and centrifuged at 4 500 r.p.m. for 30 min. Filtrate was discarded and residue on the filtration membrane was resuspended by 10 ml of 0.1 % Triton X-100 solution with pH = 12. Suspension was centrifuged again at the same conditions and residue after last centrifugation was resuspended by 10 ml of 0.1 % Triton X-100 solution (pH = 12), sonicated for 15 min again and used for next analysis.

5.5.2 Extraction by ultracentrifugation

Approximately 0.5 g of homogenized lotion was weighed to a beaker with a magnetic stir bar and 200 ml of 0.1 % Triton X-100 solution with pH = 12 was added to it. Beaker was placed on magnetic stirrer and mixed for 30 min, until homogenous white-coloured milky suspension was reached. Content of the beaker was transferred to 250 ml Teflon ultracentrifuge tube, sonicated for 15 min and centrifuged at 20 000 r.p.m. for 30 min. Supernatant after centrifugation was carefully removed by pipette and solid residue in tube was resuspended by another 200 ml volume of 0.1 % Triton X-100 solution(pH = 12).The obtained suspension was then sonicated in ultrasonic bath for 15 min. Centrifugation at the same conditions was repeated two times Residue was resuspended again in the same solution and this final suspension was after 15 min sonication used for further analysis.

Big scale extraction was done with samples number 01, 02, 05, 06, 08 and 11. In case of samples 08 and 11, hexane was used as dispersing agent. After first ultracentrifugation and hexane supernatant removal whole next procedure was identical with procedure mentioned above. All samples were done in triplicates.

5.6 Digestion procedure

Approximately 50 mg of sunscreen lotion was weighed and added into the beaker. 5 ml of hydrogen peroxide were added to the lotion. After ten minutes 10 ml of sulfuric acid was carefully added drop by drop to it and after waiting 15 min, beaker covered by watch glass was placed on hot plate.

Temperature was increased step by step to 225 °C and kept at this temperature for 1 hour. After cooling down at room temperature the content of beaker was quantitatively transferred to 100 ml volumetric flask and diluted with ultrapure water. 150 µl of the digested and diluted sample were taken and pipetted into 15 ml plastic tube and diluted with ultrapure water to a final volume of 15 ml prior to analysis using ICP-MS.

In case of determination the TiO_2 content in final suspension of extracted NPs, 10 ml of undiluted suspension was dried in beaker on hot plate at temperature 95 °C and procedure exactly identical with digestion procedure used for sunscreen lotion was applied to solid residue in the beaker.

5.7 Analytical measurements

5.7.1 HDC-ICP-MS measurement

HDC experiments were done using Agilent 1 200 HPLC system with PL-PSDA hydrodynamic-chromatography column. As an eluent 0.1 % solution of Triton X-100 with pH adjusted to 11 (NaOH) was used. The flow-rate was 2.6 $ml \cdot min^{-1}$ and the injection volume was adjusted to 30 µL of suspension. All parameters of method, except used eluent, were developed at Koblenz and Landau University.

For detecting signal ICP-MS X Series 2 system was used. However, due to unspecified problem with injection, different, lately no volumes were injected onto column and this problem was not solved even by the injection needle exchange. Therefore, no size separation using HDC was achieved in this work.

5.7.2 DLS measurements

Hydrodynamic size of the TiO_2 nanoparticles was obtained with Delsa™Nano C Particle Analyser using a laser with a wavelength of 658 nm and at a scattering angle of 165°.For the calculation of particle size distribution from autocorrelation function the CONTIN algorithm was chosen.

2 ml of sample suspension were added into polystyrene cuvettes and analyzed for 60 sec in triplicates. Summary statistics were obtained using three analyses of 1 min (total analysis time = 3 min). Instrument performance was verified using a PCS Controls reference standard supplied by manufacturer.

Average of hydrodynamic diameters of the nanoparticles were measured using DLS are listed in *Table 6*. As explained in theory, the stabilizing agent, Triton X-100 solution in this case, creates a surface layer around the primary particle and due to that hydrodynamic diameter is expected to be slightly larger than the primary particle size. The result of DLS measurements can be also affected by occurrence of particles in aggregated state in the suspension and by particle shape.

5.7.2.1 Particle concentration optimization

As was mentioned above extracted TiO_2 NPs have a strong tendency to aggregate and create large agglomerates which can be hardly considered as nanoparticles. The higher concentration of particles in suspension was, the higher agglomeration tendency and bigger agglomerates was observed. This is the reason why finding a suitable concentration, at which would particles of TiO_2 be present mainly as primary NPs, is necessary.

Stability experiment was carried out using already extracted sunscreen sample 05. Extracted suspension was diluted 10 ×, 20 ×, 50 ×, 100 ×, 200 × and 300 × in 1 % Triton X-100 solution, which is able to disagglomerate and stabilize the primary particles. Each diluted sample was bath sonicated for 15 min directly before DLS measurement.

5.7.2.2 Ultrasonic bath time optimization

Also using ultrasonication bath have to be considered to break the agglomerates of TiO_2 nanoparticles. Therefore effect of sonication and different sonication times on suspension with NPs was investigated.

For sonication time experiment suspension of extracted particles from sunscreen 05 sample was used. Sample was diluted 5× to observe suspension with particles in aggregated state and therefore, to find the proper sonication time to break most of the agglomerates. 10 ml of diluted suspension was pipetted to six 15 ml plastic tubes. Each tube was exposed in sonication bath for different time in order 0 min, 5 min, 10 min, 15 min, 20 min and 30 min. All samples were measured using DLS directly after sonication.

5.7.2.3 Stability of extracted NPs

Time stability of extracted NPs was investigated using DLS measurement by measuring the size of extracted particles two weeks after extraction. Suspensions of extracted NPs of all eleven samples were kept at laboratory temperature for two weeks. Then, suspensions were 200 × diluted with 0.1 % Triton X-100 solution with adjusted pH to 12. Samples were sonicated for 15 min and measured using DLS.

5.7.3 ICP-MS measurement

For measuring total TiO2 content in sunscreens and extracted suspensions ICP-MS X Series 2 system was used. System is equipped with a quadrupole (Thermo), PTFE spray chamber, platinum sample cone and it is thermostated with a Peltier cooler. The parameters of measurement (*table 4*) were optimized each time before analysis using a tuning solution containing Ti ions in ultrapure water. Isotopes 46Ti and 47Ti were monitored as strong interferences were observed with other isotopes.

Table 4 – typical values of system parameters for ICP-MS analysis.

Extraction	**L1**	**L2**	**QP focus**	**D1**	**D2**	**Octopole bias**
- 125 V	- 1.10 kV	- 67.5 V	9,6 V	- 45.5 V	- 140 V	- 5 V
L3	**Forward power**	**Horizontal**	**Vertical**	**DA**	**Cool**	
- 200.0 V	1.4 kW	85 mm	380 mm	- 22.0 V	13.0 °C	
Aux. gas flux	**Nebuliser gas flow**	**Hexapole bias**	**Sampling depth**	**Nebuliser Temperature**	**Dwell time**	
0.80 L/min	0.78 L/min	- 4.0 V	100 mm	3 °C	15 ms	

5.7.4 ICP-MS Calibration

A TiO_2 standard P-25 was used for preparing calibration solutions. Five calibration solutions with final concentrations 0.05, 0.1, 0.2, 0.5 and 1.0 ppm and one blank sample were prepared. Firstly the proper amount of standard for each calibration solution was weighed and added to 50 ml beaker and then it underwent digestion at the exactly same conditions as sunscreens samples. For every single measurement was always prepared new set of calibration solutions and measured new calibration curve. Linear regression was performed on the measured data.

5.7.5 SEM measurement

Scanning electron microscope was used to investigate the extracted material. Undiluted samples were pipetted onto carbon tape. Images were acquired at a beam intensity of 25-30 kV and magnification 5 000-10 000× using Quanta 250 Scanning Electron Microscope.

5.7.6 TEM measurement

The TiO_2 particle size in all sunscreen samples was determined using transmission electron microscopy. Using TEM the size and shape of particles can be reliably determined and DLS measurement can by confirmed or refuted.

Undiluted dispersions of extracted NPs were nebulized using an ultrasonic generator (system developed at the Karlsruhe Institute of Technology) onto a 3 mm copper grid covered with a combined holey and ultrathin carbon film. Measurement was done using Zeiss Leo 912 transmission electron microscope in Karlsruhe Institute of Technology. Images were acquired at beam intensity of 120 kV and magnification 20 000 ×. For each sample multiple images were collected to obtain statistically significant population of more than 200 particles. Obtained images were analyzed manually using the ImageJ software.

6. RESULTS AND DISCUSSIONS

6.1 Sample preparation

6.1.1 Solvent screening

As observed the most suitable solution for suspending sunscreens lotions was solution of Triton X-100 surfactant. Using this solution for suspending sunscreens number 01, 02, 03, 04, 05, 06 and 07 homogenous milky suspension was achieved. Ability of 0,1 % and 1 % solutions of Triton X-100 to resuspend residue after ultracentrifugation were compared and no difference was observed in final particle size. Therefore, for all future experiments 0,1 % solution was used. Water based solvents are in general less hazardous, cheaper and also closer to environmental conditions and are therefore preferred.

Also ultrapure water, ultrapure water with pH adjusted to 2 (HCl) and 12 (NaOH) and 0.1 % solution of Triton X-100 solution without and with pH adjustments to 2 (HCl) as well as 12 (NaOH) were tested for using it resuspend residues after ultracentrifugation and ultrafiltration. Ultrapure water shown weak ability to resuspend mentioned residues and big agglomerates were observed when ultrapure water was used with or without pH adjustment. Therefore, ultrapure water cannot be used as an extraction solvent. 0.1 % Triton X-100 solution and its two modifications with adjusted ph (2 and 12) shown ability to resuspend the residue. The best result was achieved using Triton X-100 solution with pH = 12, which was able to resuspend the residue easily and create homogeneous suspensions with smaller particle size. This solution was used for suspending lotion (in samples 01, 02, 03,04,05,06 and 07) and resuspending residue after ultracentrifugation or ultrafiltration steps of all sunscreen samples.

However, in cases of sunscreens 08, 09, 10 and 11 surfactant solutions were not effective to suspend/dissolve the sunscreen components and create homogenous suspension. Therefore, five organic solvents (acetone, hexane, isopropanol, tetrahydrofuran and chloroform) were tested for these samples. For further experiments hexane was chosen because of its ability to suspend and create homogenous suspension in these four sunscreen samples.

As a result of solvent screening, all eleven lotions of used sunscreens were successfully dissolved and suspended and underwent extraction procedure.

According to instability of particles in water indicates, that most of TiO_2 nanoparticles will be probably agglomerated in aquatic environment, therefore it will be adsorbed on the sludge as is mentioned above. So, there is the risk of entering TiO_2 NPs to terrestrial environment after application of sewage sludge on fields.

6.1.2 Extraction of TiO_2 nanoparticles

Two extraction methods for extracting TiO_2 NPs from sunscreen suspension were developed and applied to all mentioned sunscreen samples. The extraction methods are simple, cheap, not chemically aggresive and environmental friendly (hexane was used only in case of samples 08, 09, 10 and 11). The extraction methods, especially the ultracentrifugation one can be adapted for providing suspensions for ecotoxicological tests or fate experiments.

Following task is to determine the efficiency of these methods and determine sizes and shapes of extracted particle.

6.2 ICP-MS analysis

All raw measured data from the ICP-MS (in counts per second) were corrected by ^{103}Rh internal standard data. These corrected data were used for making calibration curves as well as for all other calculations of total TiO_2 mass, which was calculated using linear regression of calibration standards. Final mass was determined as an average of values obtained for isotopes ^{46}Ti and ^{47}Ti. Calibration curves for isotope ^{46}Ti and ^{47}Ti were prepared separately. Example of calibration curves of both isotopes with equations of linear regression are shown in *fig. 10*.

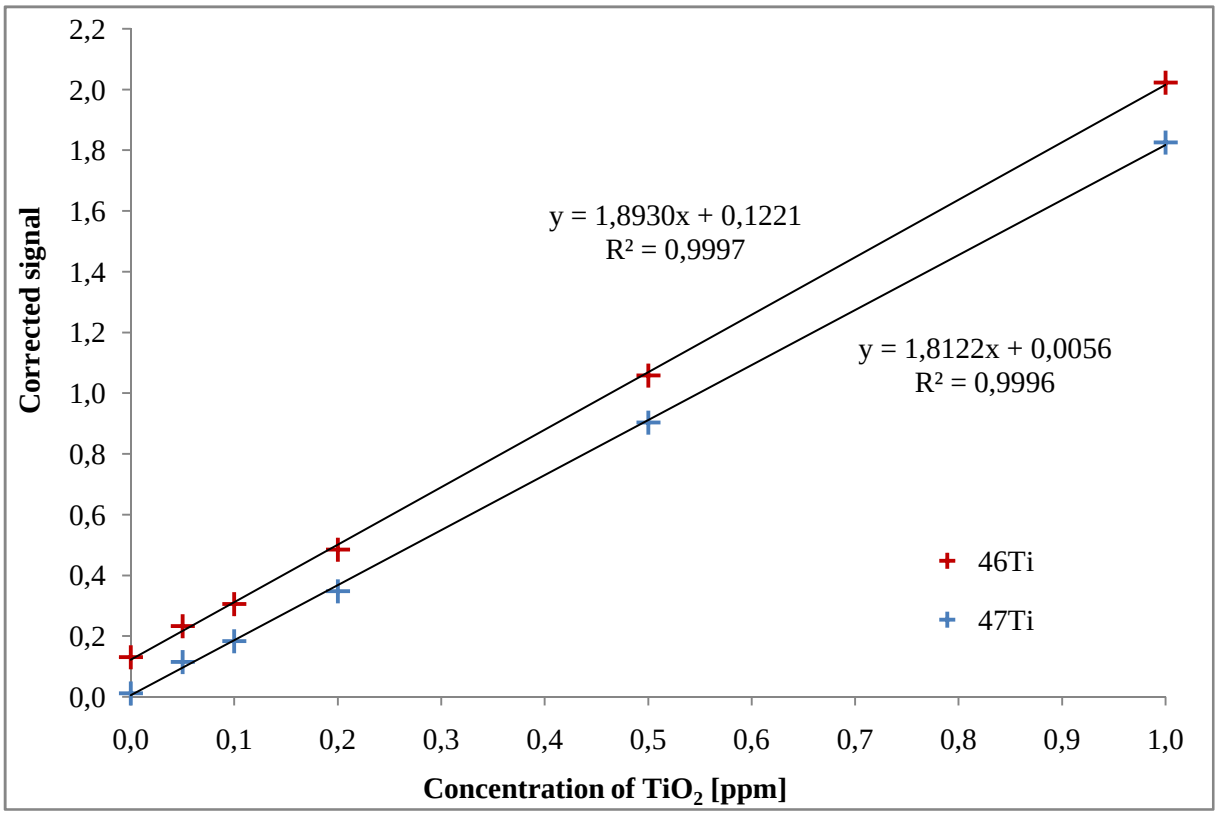

Figure 10 – example of calibration curve for isotopes ^{46}Ti and ^{47}Ti.

Results of ICP-MS measurements are shown in *table 5* and *table 6*, where we can see TiO_2 content in % obtained in sunscreen samples, final concentration of TiO_2 in extracted suspensions and determined extraction efficiencies for all eleven samples for ultrafiltration method and for six samples (01, 02, 05, 06, 08 and 11) for big scale extraction method. For comparison, bar chart of total TiO_2 mass content in all eleven sunscreens is shown in *fig. 11*.

Table 5 – total TiO_2 content, concentration of TiO_2 of final suspension and extraction efficiency of ultrafiltration.

No.	SPF	Art	TiO_2 content [mass %]	Final concentration of extracted TiO_2 [mg/l]	Extraction efficiency [%]
01	30	Spray/Lotion	4.1 ± 0.3	231 ± 31	96.0 ± 7.2
02	50+	Creme	6.1 ± 0.7	256 ± 19	73.2 ± 6.7
03	30	Lotion	5.5 ± 0.4	272 ± 17	88.2 ± 8.6
04	30	Creme	4.0 ± 0.5	210 ± 20	83.0 ± 7.4
05	50	Lotion	4.1 ± 0.2	209 ± 21	87.3 ± 6.0
06	50	Creme	5.2 ± 0.8	281 ± 24	88.2 ± 7.8
07	50	Lotion	6.0 ± 0.9	312 ± 37	73.7 ± 12.3
08	50+	Lotion	5.5 ± 0.1	272 ± 10	95.7 ± 2.3
09	30	Creme	13.1 ± 0.7	342 ± 9	51.7 ± 5.6
10	50	Creme	5.9 ± 0.2	251 ± 11	83.5 ± 7.9
11	50	Lotion	6.4 ± 0.5	239 ± 25	72.8 ± 6.3

Table 6 – total TiO_2 content, concentration of TiO_2 of final suspension and big scale extraction efficiency of ultracentrifugation.

No.	SPF	Art	TiO_2 content [%]	Final concentration of TiO_2 [mg/l]	Extraction efficiency [%]
01	30	Spray/Lotion	4.1 ± 0.3	240 ± 17	90.6 ± 5.3
02	50+	Creme	6.1 ± 0.7	375 ± 31	94.4 ± 9.2
05	50	Lotion	4.1 ± 0.2	213 ± 26	94.5 ± 7.6
06	50	Creme	5.2 ± 0.8	212 ± 12	78.0 ± 4.0
08	50+	Lotion	5.5 ± 0.1	270 ± 33	98.0 ± 6.2
11	50	Lotion	6.4 ± 0.5	308 ± 27	98.2 ± 5.4

As shown in *table 5* and *6* TiO_2 content in sunscreens was similar in ten samples (from 4,0 % to 6,4 %), and are thus in the range of what was reported in the literature (3 - 10%), except the sample 09, where TiO_2 content was considerably higher (13,1 %). The extraction efficiencies for both extraction methods are very satisfying (except for sample 09). Higher extraction efficiencies were in general obtained using ultracentrifugation extraction, which is more suitable for extracting bigger amounts of TiO_2 NPs. Uncertainty for all results was determined as standard deviation of triplicates measured.

Surprisingly, there seems to be no correlation between the SPF and the TiO_2 concentration.

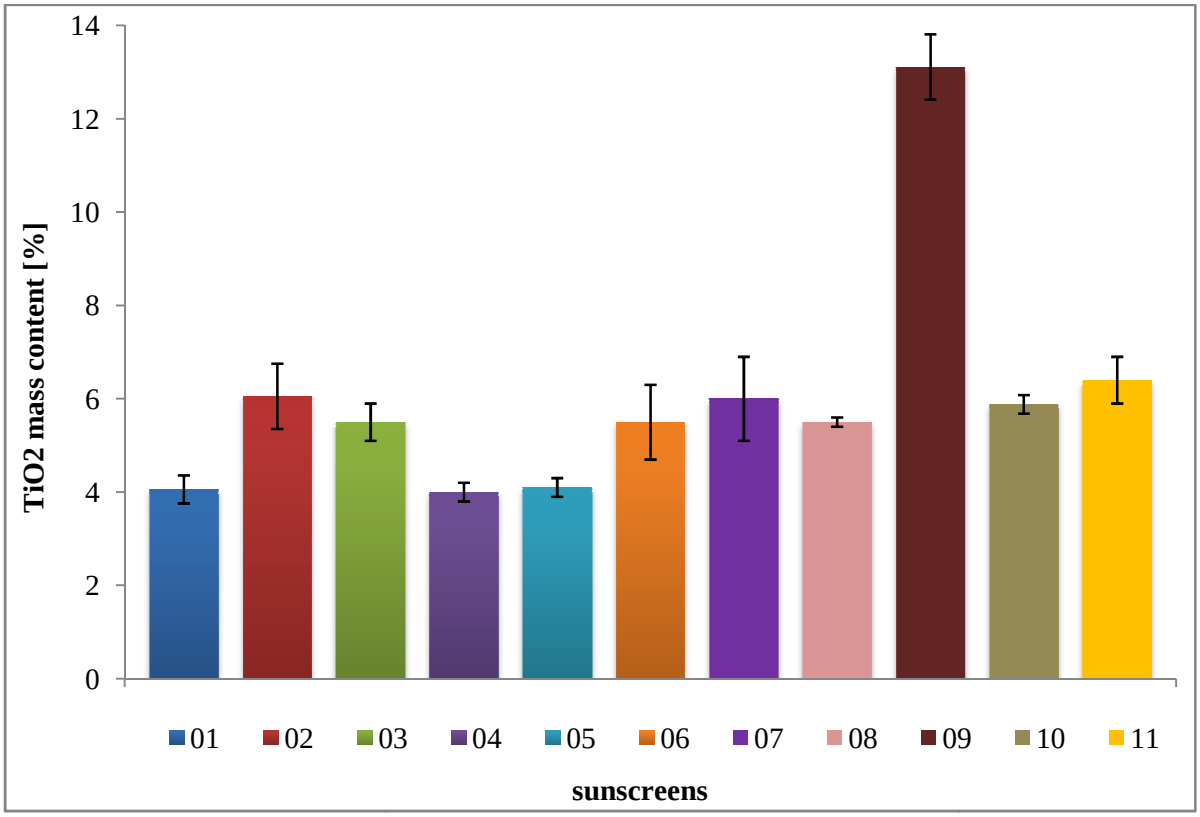

Figure 11 – comparison of TiO_2 mass content in eleven sunscreens, which were determined as average value of measured triplicates, error bars were calculated as standard deviations of triplicates.

6.3 Size analysis

6.3.1 NTA measurements

Since NTA is not capable of detecting particles smaller than about 30 nm, it was not possible to see significant fraction of TiO_2 NPs extracted from sunscreens, therefore it is not possible to determine actual size of primary nanoparticles. However, NTA can be used for investigation of presence and size distribution of agglomerates in suspensions. Thus, DLS was used in order to measure a more representative size of the extracted nanoparticles in the extracted medium.

6.3.2 DLS measurements

6.3.2.1 Particle concentration optimization

Concentration experiment confirmed that tendency of formation of aggregates in suspension with higher concentration is higher. Numerical results are shown in *table 7*. It is obvious that size of particles or agglomerates is decreasing according to higher dilution factor. From dilution 200× the size of particles or agglomerates alternatively, is constant. In case of dilution 300× the concentration was close to the detection limit of the DLS system therefore, dilution 200× was used in all next DLS measurements to observe NPs mainly in state of primary particles.

Table 7 – measured sizes of particles/agglomerates depending on dilution.

dilution	**10×**	**20×**	**50×**	**100×**	**200×**	**300×**
average	99.1	65.5	54.5	28.1	24.5	24.5
SD	3.2	2.7	2.4	1.3	1.1	1.5

6.3.2.2 Ultrasonic bath time optimization

In this experiment the effect of ultrasonication bath to break agglomerates of extracted TiO_2 NPs was studied. Diluted sample of suspension of extracted nanoparticles from sample 05 was bath sonicated for 5, 10, 15, 20 and 30 min. For control sample without being sonicated was measured too. As it is obvious, sonication significantly influenced the size of agglomerates as it is represented in *table 8*. The most suitable time of bath sonication is 15 min to obtain mostly primary particles. Size results for sunscreen number 05 differs from results shown in *table 7* and also *table 9* because of higher concentration of measured suspension in this case.

Table 8 – sizes of agglomerates in suspension according to different sonication time.

time	**0 min**	**5 min**	**10 min**	**15 min**	**20 min**	**30 min**
average	131.3	125.2	120.7	111.8	115.7	114.8
SD	7.7	5.9	4.2	4.4	3.7	4.1

6.3.2.3 Stability of extracted NPs

As is shown in *table 8* there is difference between sizes of nanoparticles determined right after extraction and size determined two weeks later are smaller than 5 % except three samples (01, 06 and 07), therefore it can be concluded, that suspensions of extracted NPs were stable in 0.1 % solution of Triton X-100 with pH = 12 in a two weeks period.

Therefore, there can be concluded, that extraction provide us stable suspension, that can be stored for at least two weeks. As is shown in *table 9*, average size of extracted particles in all sunscreen samples size approximately from 20 to 40 nm. There is also a need to determine also shape of extracted particles, which can be achieved by electron microscopy.

Table 9 – comparison of determined sizes of extracted NPs in time difference.

No.	DLS measurement		
	hydrodynamic size [nm]		difference [%]
	after extraction	after two weeks	
01	23.2 ± 1.2	24.4 ± 0.7	5.4
02	28.0 ± 1.0	28.0 ± 1.3	0.2
03	35.5 ± 2.0	34.9 ± 0.8	1.9
04	19.3 ± 0.8	19.8 ± 0.6	2.9
05	24.8 ± 0.8	24.8 ± 0.7	0.2
06	34.3 ± 0.6	32.2 ± 0.4	6.0
07	30.8 ± 1.0	27.2 ± 0.7	11.8
08	22.3 ± 0.8	22.0 ± 1.4	1.1
09	35.6 ± 0.6	36.1 ± 1.5	1.5
10	37.6 ± 1.5	38.7 ± 1.4	3.1
11	27.4 ± 1.7	27.7 ± 0.8	1.1

6.3.3 SEM measurements

Resolution of Quanta 250 Scanning Electron Microscope was insufficient to obtain primary particles of TiO_2, thus the SEM can be used to obtain images of agglomerates and study their morphology. Example of acquired image for sunscreen sample 11 is shown in *fig. 12*. Unfortunately, the SEM resolution was not sufficient for observing primary nanoparticles. Therefore, TEM was used to obtained more information of the size and morphology of the extracted nanoparticles,

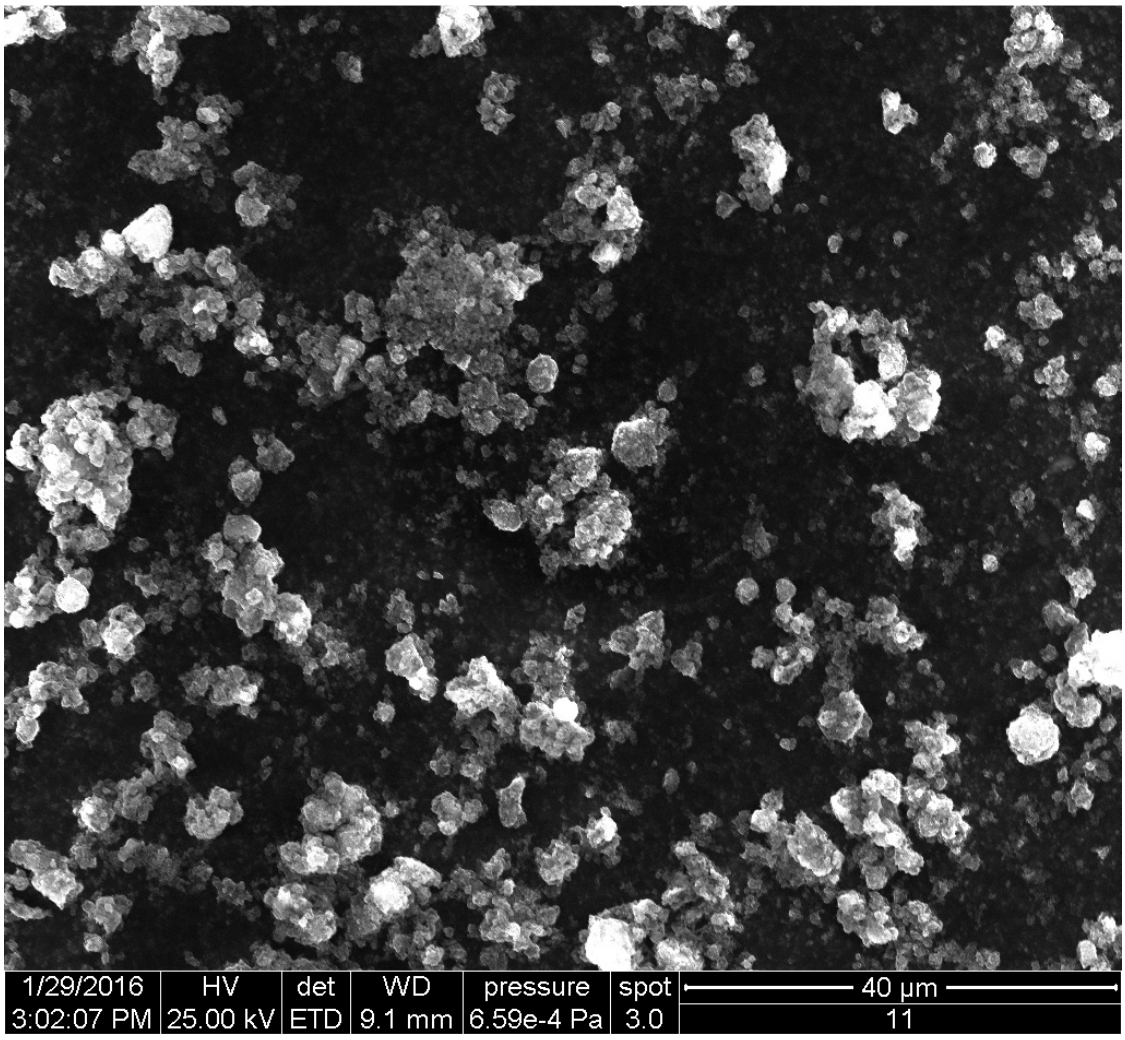

Figure 12 – example of image acquired by SEM at 25 kV beam power using ETD detector.

6.3.4 TEM measurements

According to image acquired by TEM, TiO_2 and ZnO (only in case of sample number 10) NPs differ in sunscreen samples in size and shape. Round, angular, oval as well as needle-like shaped particles or mixtures of different shaped particles were observed in the samples. Images of extracted NPs of all eleven samples are shown in *fig. 13*.

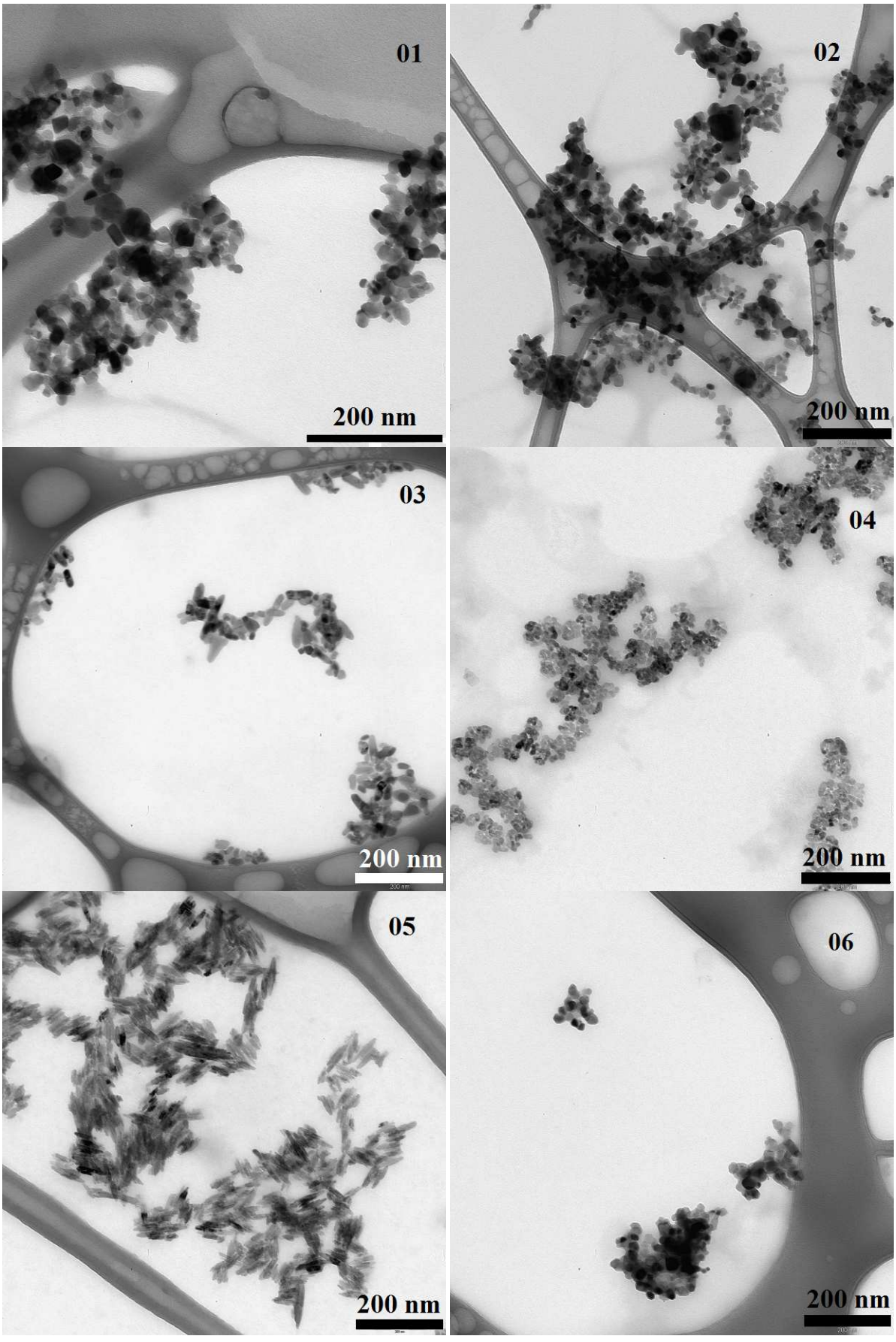
01
200 nm
02
200 nm
03
200 nm
04
200 nm
05
200 nm
06
200 nm

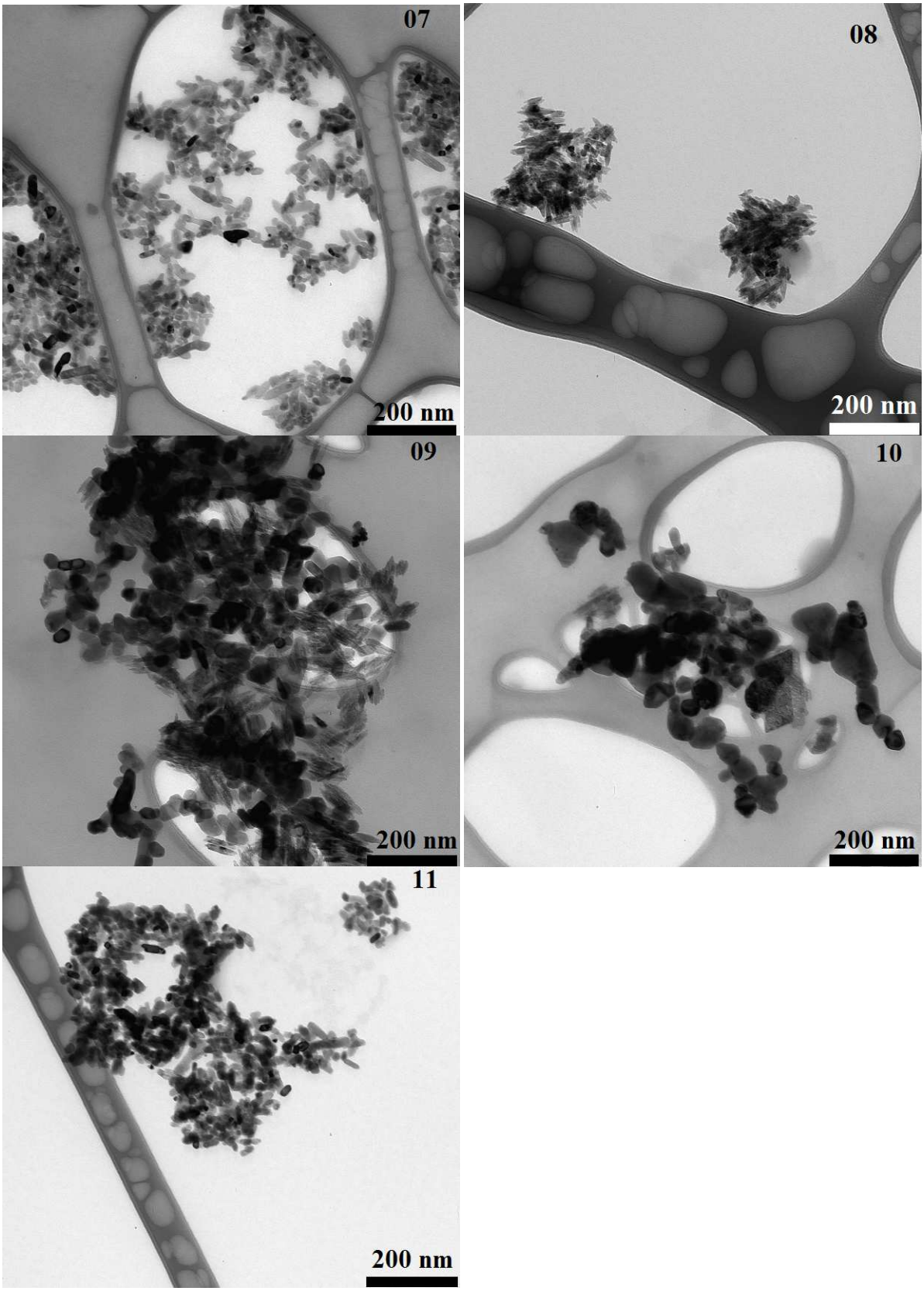

Figure 13 – representative images of extracted inorganic NPs from eleven commercial sunscreens obtained using transmission electron microscopy with copper grids. Images were acquired at a beam intensity of 120 kV and a magnification of 20 000 ×. The scale bar is 200 nm.

Table 10 – results of TEM and DLS analysis of NPs extracted from commercial sunscreens

No.	TEM measurements			DLS measurements
	average length [nm]	**average width [nm]**	**particle shape**	**hydrodynamic size [nm]**
01	19.87 ± 1.90	14.17 ± 1.50	round	23.2 ± 1.2
02	23.41 ± 1.60	14.95 ± 1.40	round and angular	28.0 ± 1.0
03	35.45 ± 2.00	15.85 ± 1.00	oval and angular	35.5 ± 2.0
04	13.37 ± 0.70	7.47 ± 0.30	round	19.3 ± 0.8
05	36.57 ± 2.80	7.31 ± 0.80	needle	24.8 ± 0.8
06	24.21 ± 1.00	15.05 ± 0.70	round	34.3 ± 0.6
07	32.48 ± 3.00	13.86 ± 0.60	oval	30.8 ± 1.0
08	29.33 ± 2.00	9.29 ± 1.80	needle, round and oval	22.3 ± 0.8
09	41.98 ± 2.90	22.70 ± 2.30	round, angular and needle	35.6 ± 0.6
10	48.83 ± 7.40	31.51 ± 5.90	round	37.6 ± 1.5
11	26.96 ± 3.00	12.37 ± 1.10	oval and round	27.4 ± 1.7

According to recommendation of European Union Commission number 2011/696/EU all sunscreen samples contain nanomaterials because one or more external dimensions of its particles are in the size range 1 – 100 nm. Based on results in *table 10* can be also concluded, that size distribution of particles obtained with DLS are comparable to sizes measured with TEM. Differences between values obtained with these two methods were expected and are caused by measuring different values. DLS method measure hydrodynamic diameter of particles, while TEM measures geometrical sizes of particles based of particle shape. Another reason of difference can be agglomeration of some of the primary particles in suspension during DLS measurement, which can increase final result.

DLS can be used as a first indication on the size but is not sufficient to describe the precise size of the particle due the complex shapes observed. However, it is very fast and simple technique for measuring size changes in suspension. To obtain precise sizes and shapes of particles TEM can be used. The TEM measurements revealed the diversity of the particle types used in these sunscreens. The variety of particle shapes let suppose a variety in phase and surface chemistry that could lead to a great variability of toxicity and fate in the environment.

Interesting fact is that size distribution is similar in all sunscreens. UV blocking activity of particles is probably size dependent and that is the reason of obtaining similar particle size distribution in all sunscreens.

On the other hand photo activity of TiO_2 as well as ability of nanoparticles to penetrate biological membranes are also size dependent. Therefore, important fact is that some of the particles were even smaller than 10 nm. There is increasing need for a complete nanotechnology risk assessment to evaluate the potential fate and indirect exposure of TiO_2 nanoparticles during their manufacturing or use, but also throughout their entire life cycle.

7. CONCLUSION

Lack of toxicological and ecotoxicological studies underlines the need for complete nanotechnology risk assessment to evaluate the potential fate and indirect exposure of complex products containing TiO_2 nanoscale structured material of different sizes and shapes and investigate their entire life cycle.

By developing two novel extraction methods for extracting TiO_2 nanoparticles from personal care products, first aim of this work was reached. Extraction methods were applied for samples of sunscreens. Since NPs are extracted directly from sunscreens, particles are more realistic in contrast to most previous studies and could be used to investigate their fate in the environment and for ecotoxicological studies applied for samples of sunscreens. The main issue is to purify these nanoparticles even from surfactant (which can interact with organisms) and stabilize these extracted NPs in the aquatic suspension to prevent them from aggregation. These investigations still have to be done before using these particles for ecotoxicological studies.

The total TiO_2 content in sunscreens and extracted suspensions was determined by ICP-MS. The final extraction efficiencies for ultrafiltration extraction in eleven sunscreens were 51,7 - 91,2 % and 78,0 - 98,2 % for ultracentrifugation extraction method in case of six samples. Ultracentrifugation method is more suitable for extracting larger amounts of TiO_2.

Sizes of extracted nanoparticles of all eleven tested sunscreens were determined by DLS. Size of particles to verify DLS results and also particle shapes was determined by TEM measurements. Sunscreens differ as in particle shapes as in size distribution of primary particles.

Although using NTA and also Quanta 250 scanning electron microscope were insufficient for determine the primary particle size, it can be used for investigation of state of agglomeration of TiO_2 nanoparticles in the suspension or morphology of agglomerate.

8. ABBREVIATIONS

3D-SEM	three-dimensional scanning electron microscopy
AFFFF-MALS	asymetrical flow field flow fractionation coupled with multi-angle light scattering
BSED	back scattered electron detector
CCD	charged coupled device
CL	cathodoluminescence
DI	deionized water
DLS or PCS	dynamic light scattering or photon correlation spectroscopy
DLS-ICP-MS	dynamic light scattering coupled with inductively coupled plasma mass spectrometry
DNA	deoxyribonucleic acid
EDS/EDX	energy dispersive spectroscopy detector
EM	electron microscopy
ETD	Everhart-Thornley detector
FCH VUT	Faculty of Chemistry, Brno University of Technology
FFF-ICP-MS	field flow fractionation coupled with inductively coupled plasma mass spectrometry
FFFF-ICP-OES	flow field flow fractionation coupled with inductively coupled plasma optical emission spectrometry
FP/FPs	fine particle/particles
GFAAS	graphite furnace atomic absorption spectroscopy
HDC	hydrodynamic chromatography
HPLC	high-performance liquid chromatography
IARC	The International Agency for Research on Cancer

ICP-MS	inductively coupled plasma mass spectrometry
ICP-OES	inductively coupled plasma optical emission spectrometry
NP/NPs	nanoparticle/nanoparticles
NTA	nanoparticle tracking analysis
QELS	quasi-elastic light scattering
RF	radio frequency
SDS	sodium dodecyl sulfate
SEC	size exclusion chromatography
SEM	scanning electron microscopy
SLS	static light scattering
SP-ICP-MS	single particle inductively coupled plasma mass spectrometry
SPF	sun protection factor
TEM	transmission electron microscopy
TMAH	tetramethylammonium hydroxide
TOF	time of flight detector
AUC	analytical ultracentrifugation
UF	ultrafiltration
US	Unites States
UV	ultra-violet
WDS	wavelength dispersive X-Ray detector
XRD	X-ray diffraction

9. REFERENCES

[1] SALATA, O. V. J. Applications of nanoparticles in biology and medicine. *Journal of Nanobiotechnology* [online]. 2 (1), 3-8 [cit. 2016-05-07]. DOI: 10.1186/1477-3155-2-3. ISSN 14773155.

[2] HOET, Peter HM, Irene BRÜSKE-HOHLFELD and O.V. J. SALATA. Nanoparticles - known and unknown health risks. *Journal of Nanobiotechnology* [online]. 2 (1), 12-22 [cit. 2016-05-07]. DOI: 10.1186/1477-3155-2-12. ISSN 14773155.

[3] CONTADO, Catia and Antonella PAGNONI. TiO2 in Commercial Sunscreen Lotion: Flow Field-Flow Fractionation and ICP-AES Together for Size Analysis. *Analytical Chemistry* [online]. 2008, 80 (19): 7594-7608 [cit. 2015-12-28]. DOI: 10.1021/ac8012626. ISSN 0003-2700.

[4] KIM, Tae-Hyun, Meeju KIM, Hyung-Seok PARK, Ueon Sang SHIN, Myoung-Seon GONG and Hae-Won KIM. Size-dependent cellular toxicity of silver nanoparticles. *Journal of Biomedical Materials Research Part A* [online]. 2012, 100 (4), 1033-1043 [cit. 2016-05-07]. DOI: 10.1002/jbm.a.34053. ISSN 15493296.

[5] JOHNSTON, Helinor J, Gary R HUTCHISON, Frans M CHRISTENSEN, Sheona PETERS, Steve HANKIN and Vicki STONE. Identification of the mechanisms that drive the toxicity of TiO2 particulates: the contribution of physicochemical characteristics. *Particle and Fibre Toxicology* [online]. 2009, 6 (1), 33- [cit. 2016-05-07]. DOI: 10.1186/1743-8977-6-33. ISSN 1743-8977.

[6] *Recommendation on the definition of a nanomaterial*. In: Brussels: European Commision, 2011, year 2011, 2011/696/EU.

[7] LORENZ, Christiane, Karen TIEDE, Steven TEAR, Alistair BOXALL, Natalie VON GOETZ and Konrad HUNGERBÜHLER. Imaging and Characterization of Engineered Nanoparticles in Sunscreens by Electron Microscopy, Under Wet and Dry Conditions. *International Journal of Occupational and Environmental Health* [online]. 2010, 16 (4), 406-428 [cit. 2016-05-07]. DOI: 10.1179/107735210799160101. ISSN 1077-3525.

[8] DAN, Yongbo, Weilan ZHANG, Runmiao XUE, Xingmao MA, Chady STEPHAN andHonglan SHI. Characterization of Gold Nanoparticle Uptake by Tomato Plants Using Enzymatic Extraction Followed by Single-Particle Inductively Coupled Plasma–Mass Spectrometry Analysis. *Environmental Science* [online]. 2015, 49 (5), 3007-3014 [cit. 2016-01-17]. DOI: 10.1021/es506179e. ISSN 0013-936x.

[9] SADRIEH, N., A. M. WOKOVICH, N. V. GOPEE, et al. Lack of Significant Dermal Penetration of Titanium Dioxide from Sunscreen Formulations Containing Nano- and Submicron-Size TiO2 Particles. *Toxicological Sciences* [online]. 2010, 115 (1), 156-166 [cit. 2016-05-08]. DOI: 10.1093/toxsci/kfq041. ISSN 1096-6080.

[10] CHUKLANOV, A. P., S. A. ZIGANSHINA and A. A. BUKHARAEV. Computer program for the grain analysis of AFM images of nanoparticles placed on a rough surface. *Surface and Interface Analysis* [online]. 2006, 38 (4), 679-681 [cit. 2016-05-08]. DOI: 10.1002/sia.2294. ISSN 0142-2421

[11] Sunscreen Explained. *The Skin Cancer Foundation* [online]. 2013 [cit. 2015-10-12].Available at: http://www.skincancer.org/prevention/sun-protection/sunscreen/sunscreens-explained

[12] Protecting Your Skin: The History of Sunscreen. *Random History* [online].2009 [cit. 2015-10-12].Available at: http://www.randomhistory.com/2009/04/28_sunscreen.html

[13] How the sun and UV cause cancer. *Cancer Research UK: Let´s beat cancer sooner* [online]. 2014 [cit. 2015-10-13]. Available at: http://www.cancerresearchuk.org/about-cancer/causes-of-cancer/sun-uv-and-cancer/how-the-sun-and-uv-cause-cancer

[14] AMARO-ORTIZ, Alexandra, Betty YAN and John D'ORAZIO. Ultraviolet Radiation, Aging and the Skin: *Prevention of Damage by Topical cAMP Manipulation. Molecules* [online]. 2014, 19 (5): 6202-6219 [cit. 2015-10-14]. DOI: 10.3390/molecules19056202. ISSN 1420-3049.

[15] Nanoparticles in Sunscreens. *EWG: Know your environment. Protect your health*. [online]. 2015 [cit. 2015-11-02].Available at: http://www.ewg.org/2015sunscreen/report/nanoparticles-in-sunscreen/

[16] SHAATH, Nadim A. *Sunscreens: regulations and commercial development*. 3rd ed. Boca Raton, Fl.: Taylor, 2005, 954 p. ISBN 08-247-5794-7.

[17] LIM, Henry W, H HÖNIGSMANN and J HAWK. *Photodermatology*. New York: Informa Healthcare USA, 2007, 472 p. ISBN 08-493-7496-0.

[18] DUPONT, E., J. GOMEZ and D. BILODEAU. Beyond UV radiation: A skin under challenge. *International Journal of Cosmetic Science* [online]. 2013, 35 (3): 224-232 [cit. 2015-10-12]. DOI: 10.1111/ics.12036. ISSN 01425463.

[19] NORDLUND, James J. *The pigmentary system: physiology and pathophysiology*. 2nd ed. Malden, Mass.: Blackwell Pub., 2006, 1229 p. ISBN 14-051-2034-7.

[20] Sunburn Protection Factor (SPF). *U.S. Food and Drug Administration: Protecting and promoting your health* [online]. 2009 [cit. 2015-12-28]. Available at: http://www.fda.gov/aboutfda/centersoffices/officeofmedicalproductsandtobacco/cder/ucm106351.htm

[21] What is SPF Sunscreen? *Badger: HealthyBody Care* [online]. 2008 [cit. 2015-12-28]. Available at: http://www.badgerbalm.com/s-30-what-is-spf-sunscreen-sun-protection-factor.aspx

[22] VENDITTI, Elisabetta, Francesca BRUGÈ, Paola ASTOLFI, Irene KOCHEVAR and Elisabetta DAMIANI. Nitroxides and a nitroxide-based UV filter have the potential to photoprotect UVA-irradiated human skin fibroblasts against oxidative damage. *Journal of Dermatological Science* [online]. 2011, 63 (1): 55-61 [cit. 2015-10-14]. DOI: 10.1016/j.jdermsci.2011.03.008. ISSN 09231811.

[23] LABILLE, Jérôme, Jinghuan FENG, Céline BOTTA, et al. Aging of TiO2 nanocomposites used in sunscreen. Dispersion and fate of the degradation products in aqueous environment.*Environmental Pollution* [online]. 2010, 158 (12), 3482-3489 [cit. 2016-05-02]. DOI: 10.1016/j.envpol.2010.02.012. ISSN 02697491.

[24] KRAUSE, M., A. KLIT, M. BLOMBERG JENSEN, T. SØEBORG, H. FREDERIKSEN, M. SCHLUMPF, W. LICHTENSTEIGER, N. E. SKAKKEBAEK and K. T. DRZEWIECKI. Sunscreens: are they beneficial for health? An overview of endocrine disrupting properties of UV-filters.*International Journal of Andrology* [online]. 2012, 35 (3): 424-436 [cit. 2015-11-02]. DOI: 10.1111/j.1365-2605.2012.01280.x. ISSN 01056263.

[25] JANJUA, NR, B KONGSHOJ, A-M ANDERSSON and HC WULF. Sunscreens in human plasma and urine after repeated whole-body topical application. *Journal of the European Academy of Dermatology and Venereology* [online]. 2008, 22 (4): 456-461 [cit. 2015-11-02]. DOI: 10.1111/j.1468-3083.2007.02492.x. ISSN 0926-9959.

[26] KLINUBOL, P., P. ASAWANONDA, S.P. WANICHWECHARUNGRUANG and B. MURPHY. Transdermal Penetration of UV Filters. *Skin Pharmacology and Physiology* [online]. 2008, 21 (1): 23-29 [cit. 2015-11-02]. DOI: 10.1159/000109085. ISSN 1660-5535.

[27] SARVEIYA, Vikram, Stacey RISK, Heather A.E BENSON and B. MURPHY. Liquid chromatographic assay for common sunscreen agents: application to in vivo assessment of skin penetration and systemic absorption in human volunteers. *Journal of Chromatography B* [online]. 2004, 803 (2): 225-231 [cit. 2015-11-02]. DOI: 10.1016/j.jchromb.2003.12.022. ISSN 15700232.

[28] SHAW, Daniel W. Allergic Contact Dermatitis from Octisalate and cis-3-Hexenyl Salicylate. *Dermatitis* [online].2006,17 (3): 152-155 [cit. 2015-11-02]. DOI: 10.2310/6620.2006.05046. ISSN 1710-3568.

[29] BRYDEN, Pamela J. and E.A. ROY. Preferential reaching across regions of hemispace in adults and children. *Developmental Psychobiology* [online]. 2006, 48 (2): 121-132 [cit. 2015-11-02]. DOI: 10.1002/dev.20120. ISSN 0012-1630.

[30] GAMER, A.O., E. LEIBOLD and B. VAN RAVENZWAAY. The in vitro absorption of microfine zinc oxide and titanium dioxide through porcine skin. *Toxicology in Vitro* [online]. 2006, 20 (3): 301-307 [cit. 2015-11-02]. DOI: 10.1016/j.tiv.2005.08.008. ISSN 08872333.

[31] SADRIEH, N., A. M. WOKOVICH, N. V. GOPEE, J. ZHENG, D. HAINES, D. PARMITER, P. H. SIITONEN, C. R. COZART, A. K. PATRI, et al. Lack of Significant Dermal Penetration of Titanium Dioxide from Sunscreen Formulations Containing Nano- and Submicron-Size TiO2 Particles. *Toxicological Sciences* [online]. 2010, 115 (1): 156-166 [cit. 2015-11-02]. DOI: 10.1093/toxsci/kfq041. ISSN 1096-6080.

[32] SAYES, C. M., K. L. REED and D. B. WARHEIT.Assessing Toxicity of Fine and Nanoparticles: Comparing In Vitro Measurements to In Vivo Pulmonary Toxicity Profiles. *Toxicological Science s*[online]. 2007, 97 (1): 163-180 [cit. 2015-11-02]. DOI: 10.1093/toxsci/kfm018. ISSN 1096-6080.

[33] LANDMANN, M, E RAULS and W G SCHMIDT.The electronic structure and optical response of rutile, anatase and brookite TiO2. *Journal of Physics*: *Condensed Matter* [online]. 2012, 24 (19): 195503- [cit. 2015-11-28]. DOI: 10.1088/0953-8984/24/19/195503. ISSN 0953-8984.

[34] GUPTA, Shipra Mitaland Manoj TRIPATHI. A review of TiO2 nanoparticles. Chinese *Science Bulletin* [online]. 2011, 56 (16): 1639-1657 [cit. 2015-11-28]. DOI: 10.1007/s11434-011-4476-1. ISSN 1001-6538.

[35] DIEBOLD, U. Structure and properties of TiO2 surfaces: a brief review. *Applied Physics A: Materials Science* [online]. 2003, 76 (5): 681-687 [cit. 2015-11-28]. DOI: 10.1007/s00339-002-2004-5. ISSN 0947-8396.

[36] *Nanoparticle technology handbook*. 2nd ed. Amsterdam: Elsevier, 2012, xxv, 703 p. ISBN 978-0-444-56336-1.

[37] What is nanotechnology? *Nano: National Nanotechnology Initiative* [online]. 2013 [cit. 2015-11-09].Available at: http://www.nano.gov/nanotech-101/what/definition

[38] COLE, James L., Jeffrey W. LARY, Thomas P. MOODY and Thomas M. LAUE. Analytical Ultracentrifugation: Sedimentation Velocity and Sedimentation Equilibrium. *Methods of Cell Biology* [online]. 2009, (84): 143 [cit. 2015-11-11]. DOI: 10.1016/S0091-679X(07)84006-4.

[39] WEITHÖNER, Frank. Laboratory Centrifuges. *Frank´s Hospital Workshop* [online]. 2014 [cit. 2015-11-11]. Available at: http://www.frankshospitalworkshop.com/equipment/centrifuges_equipment.html

[40] CHEN, Sheng-Chieh, Doris SEGETS, Tsz-Yan LING, Wolfgang PEUKERT and David Y.H. PUI.An experimental study of ultrafiltration for sub-10nm quantum dots and sub-150 nm nanoparticles through PTFE membrane and Nucleporefilters. *Journal of Membrane Science* [online]. 2015, (497): 153-161 [cit. 2015-11-11]. DOI: 10.1016/j.memsci.2015.09.022. ISSN 03767388.

[41] GARAJ, Ján, Dušan BUSTIN and Zdeněk HLADKÝ. *Analytická chémia: celoštátna vysokoškolská učebnica pre chemickotechnologické fakulty vysokých škôl*. Bratislava: Alfa, 1987, 740 p.

[42] NOVÁKOVÁ, Lucie and Michal DOUŠA. *Moderní HPLC separace v teorii a praxi*. 1st ed. Hradec Králové, Klatovy: Lucie Nováková, Michal Douša, 2013, 299 p. ISBN 978-80-260-4243-3.

[43] CHURÁČEK, Jaroslav. *Analytická separace látek*. 1st ed. Praha: SNTL, 1990, 384 p. ISBN 80-030-0569-8.

[44] IDEX Corporation. Unchurp: HPLC Center. *IDEX Health & Science*. [online]. 2014 [cit. 2014-04-14].Available at: http://www.idexhs.com/support/upchurch/hplc_center.aspx

[45] WILCOXON, J. P., J. E. MARTIN and P. PROVENCIO.Size Distributions of Gold Nanoclusters Studied by Liquid Chromatography. *Langmuir* [online]. 2000, 16 (25): 9912-9920 [cit. 2016-01-04]. DOI: 10.1021/la000669j. ISSN 0743-7463.

[46] JIMENEZ, Victoria L., Michael C. LEOPOLD, Carolyn MAZZITELLI, James W. JORGENSON and Royce W. MURRAY.HPLC of Monolayer-Protected Gold Nanoclusters. *Analytical Chemistry* [online]. 2003, 75 (2): 199-206 [cit. 2016-01-04]. DOI: 10.1021/ac0260589. ISSN 0003-2700.

[47] KOWALCZYK, Bartlomiej, István LAGZI and Bartosz A. GRZYBOWSKI. Nanoseparations: Strategies for size and/or shape-selective purification of nanoparticles. *Current Opinion in Colloid* [online]. 2011, 16 (2): 135-148 [cit. 2016-01-04]. DOI: 10.1016/j.cocis.2011.01.004. ISSN 13590294.

[48] REVILION, A. Hydrodynamic Chromatography. *Centre National de la Recherche Scientifique* [online]. 2000, (24) [cit. 2016-03-26].

[49] MALYSHEVA, Anzhela, Enzo LOMBI and Nicolas H. VOELCKER.Bridging the divide between human and environmental nanotoxicology. *Nature Nanotechnology* [online]. 2015, (10), 835-844 [cit. 2016-03-26]. DOI: 10.1038/nnano.2015.224. ISSN 1748-3387.

[50] CHANG, Ying-jie, Yang-hsin SHIH, Chiu-Hun SU and Han-Chen HO. Comparison of Three Analytical Methods to Measure the Size of Silver Nanoparticles in Real Environmental Water and Wastewater Samples. *Journal of Hazardous Materials* [online]. 2016, (302), [cit. 2016-03-26]. DOI: 10.1016/j.jhazmat.2016.03.030. ISSN 03043894.

[51] PERGANTIS, Spiros A., Tammy L. JONES-LEPP and Edward M. HEITHMAR. Hydrodynamic Chromatography Online with Single Particle-Inductively Coupled Plasma Mass Spectrometry for Ultratrace Detection of Metal-Containing Nanoparticles. *Analytical Chemistry* [online]. 2012, 84 (15), 6454-6462 [cit. 2016-03-26]. DOI: 10.1021/ac300302j. ISSN 0003-2700.

[52] ØGENDA, Lars. *Light scattering: a brief introduction* [online]. University of Copenhagen, 2015, 42 p. [cit. 2015-01-03].

[53] BRAR, Satinder K. and M. VERMA.Measurement of nanoparticles by light-scattering techniques. *TrAC Trends in Analytical Chemistry* [online]. 2011, 30 (1): 4-17 [cit. 2016-01-03]. DOI: 10.1016/j.trac.2010.08.008. ISSN 01659936.

[54] Dynamic light scattering: Common terms defined. Malvern Instruments Worldwide [online]. Worcestershire: Malvern Instruments Limited, 2011 [cit. 2016-04-16].

[55] Dynamic Light Scattering: An Introduction in 30 Minutes. *Malvern* [online]. Malvern: Malvern Instruments Ltd, 2009 [cit. 2016-04-18]. Available at: http://www.malvern.com/en/support/resource-center/technical-notes/TN101104DynamicLightScatteringIntroduction.aspx

[56] BODYCOMB, Jeffrey. Interpreting and Understanding Dynamic Light Scattering Data. *HORIBA Scientific* [online]. Kyoto: Horiba, 2012 [cit. 2016-04-18].

[57] Dynamic Light Scattering: Measuring the Particle Size Distribution. *LS Instruments* [online]. 2015 [cit. 2016-03-12].

[58] Characterizing Exosomes and Microvesicles with Nanoparticle Tracking Analysis. *News Medical: life science and Medicine* [online]. Worcestershire: News Medical, 2015 [cit. 2016-05-04]. Available at: http://www.news-medical.net/whitepaper/20150914/Characterizing-Exosomes-and-Microvesicles-with-Nanoparticle-Tracking-Analysis.aspx

[59] GROSS, Julia, Sabrina SAYLE, Anne R. KAROW, Udo BAKOWSKY and Patrick GARIDEL. Nanoparticle tracking analysis of particle size and concentration detection in suspensions of polymer and protein samples: Influence of experimental and data evaluation parameters. *European Journal of Pharmaceutics and Biopharmaceutics* [online]. 2016, 104, 30-41 [cit. 2016-05-04]. DOI: 10.1016/j.ejpb.2016.04.013. ISSN 09396411.

[60] SALVADOR, A., M.C. PASCUAL-MARTÍ, J.R. ADELL, A. REQUENI and J.G. MARCH. Analytical methodologies for atomic spectrometric determination of metallic oxides in UV sunscreen creams. *Journal of Pharmaceutical and Biomedical Analysis* [online]. 2000, 22 (2): 301-306 [cit. 2016-01-04]. DOI: 10.1016/S0731-7085(99)00286-1. ISSN 07317085.

[61] BAIRI, Venu Gopal, Jin-Hee LIM, Ivan R. QUEVEDO, Thilak K. MUDALIGE and Sean W. LINDER. Portable X-ray fluorescence spectroscopy as a rapid screening technique for analysis of TiO2 and ZnO in sunscreens. *Spectrochimica Acta Part B: Atomic Spectroscopy* [online]. 2016, (116): 21-27 [cit. 2016-01-04]. DOI: 10.1016/j.sab.2015.11.008. ISSN 05848547.

[62] ZACHARIADIS, G.A. and E. SAHANIDOU.Multi-element method for determination of trace elements in sunscreens by ICP-AES. *Journal of Pharmaceutical and Biomedical Analysis* [online]. 2009, 50 (3): 342-348 [cit. 2016-01-04]. DOI: 10.1016/j.jpba.2009.05.003. ISSN 07317085.

[63] CUDDY, Michael F, Aimee R PODA, Robert D MOSER, Charles A WEISS, Carolyn CAIRNS and Jeffery A STEEVENS. A weight-of-evidence approach to identify nanomaterials in consumer products: a case study of nanoparticles in commercial sunscreens. *Journal of Exposure Science and Environmental Epidemiology* [online]. 2015, 26 (1): 26-34 [cit. 2015-12-28]. DOI: 10.1038/jes.2015.51. ISSN 1559-0631.

[64] LÓPEZ-HERAS, Isabel, Yolanda MADRID and Carmen CÁMARA. Prospects and difficulties in TiO2 nanoparticles analysis in cosmetic and food products using asymmetrical flow field-flow fractionation hyphenated to inductively coupled plasma mass spectrometry. *Talanta* [online]. 2014, (124): 71-78 [cit. 2016-01-04]. DOI: 10.1016/j.talanta.2014.02.029. ISSN 00399140.

[65] What is ICP-MS?: and more importantly, what can it do? WOLF, Ruth E. *USGS Crustal Geophysics and Geochemistry Science Center* [online].2005 [cit. 2015-11-23].Available at: http://crustal.usgs.gov/laboratories/icpms/intro.html

[66] Inductively-Coupled Plasma (ICP) Excitation Source. Science Hypermedia [online]. 1996 [cit. 2015-11-23]. Available at: https://www.uam.es/docencia/quimcursos/Scimedia/chem-ed/spec/atomic/emission/icp.htm

[67] Reviews in mineralogy and geochemistry. Geo science world [online]. 2012 [cit. 2015-11-23].Available at: http://rimg.geoscienceworld.org/content/53/1/243/F4.expansion.html

[68] HOU, Xiandeng and Bradley T. JONES. Inductively Coupled Plasma/Optical Emission Spectrometry. *Encyclopedia of Analytical Chemistry* [online]. 2000, (3) [cit. 2016-01-04].

[69] What is Electron Microscopy? *John Innes Centre* [online]. 2011 [cit. 2015-12-05].Available at: https://www.jic.ac.uk/microscopy/intro_EM.html

[70] An Introduction to Electron Microscopy. *FEI* [online]. 2015 [cit. 2015-12-05]. Available at: http://www.fei.com/introduction-to-electron-microscopy/

[71] How an SEM Works. *Nano Science Instruments* [online]. 2009 [cit. 2015-12-05].Available at: http://www.nanoscience.com/products/sem/technology-overview/how-sem-works/

[72] SEM Component Details. Michigen State University. *Chemical Engineering and Material Science* [online].2010 [cit. 2016-02-08]. Available at: http://www.chems.msu.edu/resources/tutorials/SEM/component-details

[73] Scanning Electron Microscope (SEM): Everhart Thornley detector. University of Liverpool. *Introduction to Electron Microscopes* [online]. 2007 [cit. 2016-02-07].Available at: http://www.materials.ac.uk/elearning/matter/introductiontoelectronmicroscopes/sem/everhart.html

[74] Backscattered electron detector (BSD) – solid state diode detector. *My Scope: Training for advanced research* [online]. 2012 [cit. 2016-02-08].Available at: http://li155-94.members.linode.com/myscope/sem/background/whatissem/detectors.php

[75] Energy-Dispersive X-Ray Spectroscopy (EDS). *Science Education Research Center Carleton* [online]. 2007 [cit. 2016-02-08]. Available at: http://serc.carleton.edu/research_education/geochemsheets/eds.html

[76] Preparing samples for the electron microscope. *Science learning: Sparking fresh thinking* [online]. 2012 [cit. 2015-12-06]. Available at: http://sciencelearn.org.nz/Contexts/Exploring-with-Microscopes/Looking-Closer/Preparing-samples-for-the-electron-microscope

[77] SHI, Hongbo, Ruth MAGAYE, Vincent CASTRANOVA andJinshun ZHAO. Titanium dioxide nanoparticles: a review of current toxicological data. *Particle and Fibre Toxicology* [online].2013, 10 (1): 15 [cit. 2015-11-11]. DOI: 10.1186/1743-8977-10-15. ISSN 1743-8977.

[78] NG, Cheng-Teng, Jasmine J. LI, Boon-Huat BAY and Lin-Yue LanryYUNG.Current Studies into the Genotoxic Effects of Nanomaterials. *Journal of Nucleic Acids* [online]. 2010, (2010): 1-12 [cit. 2015-11-23]. DOI: 10.4061/2010/947859. ISSN 2090-021x.

[79] LADEMANN, Juergen, Hans-Juergen WEIGMANN, Christiane RICKMEYER, Hans BARTHELMES, Hans SCHAEFER, Gerhard MUELLER and Wolfram STERRY. Penetration of Titanium Dioxide Microparticles in a Sunscreen Formulation into the Horny Layer and the Follicular Orifice. *Skin Pharmacology and Physiology* [online]. 1999, 12 (5): 247-256 [cit. 2015-11-11]. DOI: 10.1159/000066249. ISSN 1660-5535.

[80] MAVON, A., C. MIQUEL, O. LEJEUNE, B. PAYRE and P. MORETTO. In vitro Percutaneous Absorption and in vivo Stratum Corneum Distribution of an Organic and a Mineral Sunscreen. *Skin Pharmacology and Physiology* [online]. 2007, 20 (1): 10-20 [cit. 2015-11-11]. DOI: 10.1159/000096167. ISSN 1660-5535.

[81] POPOV, Alexey P., Alexander V. PRIEZZHEV, Jürgen LADEMANN and Risto MYLLYLÄ. Alteration of skin light-scattering and absorption properties by application of sunscreen nanoparticles: A Monte Carlo study. *Journal of Quantitative Spectroscopy and Radiative Transfer* [online]. 2011, 112 (11): 1891-1897 [cit. 2015-11-11]. DOI: 10.1016/j.jqsrt.2011.01.015. ISSN 00224073.

[82] DUNFORD, Rosemary, Angela SALINARO, Lezhen CAI, Nick SERPONE, Satoshi HORIKOSHI, Hisao HIDAKA and John KNOWLAND. Chemical oxidation and DNA damage catalysed by inorganic sunscreen ingredients. *FEBS Letters* [online]. 1997, 418 (1-2), 87-90 [cit. 2016-02-21]. DOI: 10.1016/S0014-5793(97)01356-2. ISSN 00145793.

[83] TSUJI, J. S. Research Strategies for Safety Evaluation of Nanomaterials, Part IV: Risk Assessment of Nanoparticles. *Toxicological Sciences* [online]. 2005, 89 (1), 42-50 [cit. 2016-02-21]. DOI: 10.1093/toxsci/kfi339. ISSN 1096-6080.

[84] JOHNSON, Andrew C., Michael J. BOWES, Alison CROSSLEY, Helen P. JARVIE, Kerstin JURKSCHAT, Monika D. JÜRGENS, Alan J. LAWLOR, Barry PARK, Phillip ROWLAND, et al. An assessment of the fate, behaviour and environmental risk associated with sunscreen TiO2 nanoparticles in UK field scenarios. *Science of The Total Environment* [online]. 2011,409 (13): 2503-2510 [cit. 2015-11-22]. DOI: 10.1016/j.scitotenv.2011.03.040. ISSN 00489697.

[85] BOTTA, Céline, Jérôme LABILLE, Mélanie AUFFAN, Daniel BORSCHNECK, Hélène MICHE, Martiane CABIÉ, Armand MASION, Jérôme ROSE and Jean-Yves BOTTERO. TiO2-based nanoparticles released in water from commercialized sunscreens in a life-cycle perspective: Structures and quantities.*Environmental Pollution* [online]. 2011, 159 (6): 1543-1550 [cit. 2015-11-22]. DOI: 10.1016/j.envpol.2011.03.003. ISSN 02697491.

[86] WARHEIT, D, R HOKE, C FINLAY, E DONNER, K REED and C SAYES. Development of a base set of toxicity tests using ultrafine TiO2 particles as a component of nanoparticle risk management. *Toxicology Letters* [online]. 2007, 171(3): 99-110 [cit. 2015-11-23]. DOI: 10.1016/j.toxlet.2007.04.008. ISSN 03784274.

[87] PAN, Xiaoping, James E. REDDING, Patricia A. WILEY, Lisa WEN, J. Scott MCCONNELL andBaohong ZHANG. Mutagenicity evaluation of metal oxide nanoparticles by the bacterial reverse mutation assay. *Chemosphere* [online]. 2010, 79 (1): 113-116 [cit. 2015-11-23]. DOI: 10.1016/j.chemosphere.2009.12.056. ISSN 00456535.

[88] KUMAR, Ashutosh, Alok K. PANDEY, Shashi S. SINGH, Rishi SHANKER and Alok DHAWAN.Cellular uptake and mutagenic potential of metal oxide nanoparticles in bacterial cells. *Chemosphere* [online]. 2011, 83 (8): 1124-1132 [cit. 2015-11-23]. DOI: 10.1016/j.chemosphere.2011.01.025. ISSN 00456535.

[89] PODA, A.R., A.J. BEDNAR, A.J. KENNEDY, A. HARMON, M. HULL, D.M. MITRANO, J.F. RANVILLE and J. STEEVENS. Characterization of silver nanoparticles using flow-field flow fractionation interfaced to inductively coupled plasma mass spectrometry. *Journal of Chromatography A* [online]. 2011, 1218 (27), 4219-4225 [cit. 2016-01-12]. DOI: 10.1016/j.chroma.2010.12.076. ISSN 00219673.

[90] SCHMIDT, Bjørn, Katrin LOESCHNER, Niels HADRUP, Alicja MORTENSEN, Jens J. SLOTH, Christian BENDER KOCH and Erik H. LARSEN. Quantitative Characterization of Gold Nanoparticles by Field-Flow Fractionation Coupled Online with Light Scattering Detection and Inductively Coupled Plasma Mass Spectrometry. *Analytical Chemistry* [online]. 2011, 83 (7), 2461-2468 [cit. 2016-01-12]. DOI: 10.1021/ac102545e. ISSN 0003-2700.

[91] GRAY, Evan P., Jessica G. COLEMAN, Anthony J. BEDNAR, Alan J. KENNEDY, James F. RANVILLE and Christopher P. HIGGINS. Extraction and Analysis of Silver and Gold Nanoparticles from Biological Tissues Using Single Particle Inductively Coupled Plasma Mass Spectrometry. *Environmental Science* [online]. 2013, 47 (24), 14315-14323 [cit. 2016-01-17]. DOI: 10.1021/es403558c. ISSN 0013-936x.

[92] KRYSTEK, Petra, Sicco BRANDSMA, Pim LEONARDS and Jacob DE BOER. Exploring methods for compositional and particle size analysis of noble metal nanoparticles in Daphnia magna. *Talanta* [online]. 2016, 147 (9), 289-295 [cit. 2016-01-17]. DOI: 10.1016/j.talanta.2015.09.063. ISSN 00399140.

[93] LOESCHNER, Katrin, Jana NAVRATILOVA, Carsten KØBLER, Kristian MØLHAVE, Stephan WAGNER, Frank VON DER KAMMER and Erik H. LARSEN. Detection and characterization of silver nanoparticles in chicken meat by asymmetric flow field flow fractionation with detection by conventional or single particle ICP-MS. *Analytical and Bioanalytical Chemistry* [online]. 2013, 405 (25), 8185-8195 [cit. 2016-01-17]. DOI: 10.1007/s00216-013-7228-z. ISSN 1618-2642.

[94] WHITLEY, Annie R., Clément LEVARD, Emily OOSTVEEN, Paul M. BERTSCH, Chris J. MATOCHA, Frank von der KAMMER and Jason M. UNRINE. Behavior of Ag nanoparticles in soil: Effects of particle surface coating, aging and sewage sludge amendment. *Environmental Pollution* [online]. 2013, 182 (27), 141-149 [cit. 2016-01-17]. DOI: 10.1016/j.envpol.2013.06.027. ISSN 02697491.

[95] NISCHWITZ, Volker and Heidi GOENAGA-INFANTE. Improved sample preparation and quality control for the characterisation of titanium dioxide nanoparticles in sunscreens using flow field flow fractionation on-line with inductively coupled plasma mass spectrometry. *Journal of Analytical Atomic Spectrometry* [online]. 2012, 27(7): 1084[cit. 2015-12-28]. DOI: 10.1039/c2ja10387g. ISSN 0267-9477.

[96] LEWICKA, Zuzanna A., Angelo F. BENEDETTO, Denise N. BENOIT, William W. YU, John D. FORTNER and Vicki L. COLVIN. The structure, composition, and dimensions of TiO2 and ZnO nanomaterials in commercial sunscreens. *Journal of Nanoparticle Research* [online]. 2011, 13(9): 3607-3617 [cit. 2015-12-28]. DOI: 10.1007/s11051-011-0438-4. ISSN 1388-0764.

[97] Research Unit INTERNANO. *University of Koblenz and Landau* [online]. Landau: University of Koblenz and Landau, 2011 [cit. 2016-05-05]. Available at: https://www.uni-koblenz-landau.de/de/landau/fb7/umweltwissenschaften/forschung/internano/internano_content